Spring 1976

THE MEASUREMENT OF (NUCLEAR G-FACTOR OF UNIPOSITIVE SODIUM-23 ION)/(ELECTRONIC G-FACTOR OF SODIUM-23) BY OPTICAL PUMPING

CHUNG-JEN TSAI

THE MEASUREMENT OF $g_I(^{23}Na^+)/g_J(^{23}Na)$ BY OPTICAL PUMPING

by

CHUNG-JEN TSAI

B.S., Cheng Kung University, Taiwan, China, 1964

M.S., University of New Hampshire, 1971

A THESIS

Submitted to the University of New Hampshire

In partial Fulfillment of

The Requirements for the Degree of

Doctor of Philosophy

Graduate School

Department of Physics

May, 1976

This thesis has been examined and approved

Ludwig C. Balling

Thesis Director, Ludwig C. Balling, Prof. of Physics

Richard L. Kaufmann, Prof. of Physics

Robert H. Lambert, Prof. of Physics

John E. Mulhern, Jr., Prof. of Physics

John J. Wright, Asst. Prof. of Physics

April 14, 1976

Date

ACKNOWLEDGEMENTS

I wish to express my deepest gratitude to my thesis advisor, Professor L. C. Balling, who has provided me not only the opportunity to work on the problem, but also continuous guidance, encouragement and support. I also wish to thank Dr. J. J. Wright, Dr. R. H. Lambert, Dr. J. E. Mulhern, Jr., and Dr. R. L. Kaufmann, for their critical reading, and many helpful discussion and comments.

I am also indebted to James E. Williams, Arthur L. Anderson, and Albert W. Knight for their invaluable technical support.

Finally, I would like to acknowledge the debt owed to my wife, Kuei-Fang, for her typing of this thesis, and for her patience, understanding as well as continual loyal support.

This work was supported in part by the National Science Foundation under contracts NSF-GP-43615.

TABLE OF CONTENTS

LIST OF TABLES

LIST OF ILLUSTRATIONS

ABSTRACT

THE MEASUREMENT OF $g_I(^{23}Na^+)/g_J(^{23}Na)$
BY OPTICAL PUMPING

by

CHUNG-JEN TSAI

A charge-exchange Optical-Pumping experiment has been performed to measure the ratio $g_I(^{23}Na^+)/g_J(^{23}Na)$. The NMR frequency of free $^{23}Na^+$ ions polarized by charge-exchange collisions with optically pumped ^{23}Na atoms was measured along with the ($F = 2, M = -2 \leftrightarrow F = 2, M = -1$) Zeeman transition frequency of ^{23}Na in a magnetic field of ~ 57 Gauss. The magnetic field was produced in a shielded solenoid. The 300-cm^3 spherical cells were filled with ~ 150 Torr of Ne buffer gas, and the ions were produced by rf discharge with a pair of electrodes, which were run in the turrets attached to the cells. The NMR frequency was ~ 61 KHz. The charge-exchange and rf broadened NMR linewidth was ~ 250 Hz. The Zeeman frequency was ~ 40 MHz and the Zeeman linewidth was ~ 400 Hz due to the inhomogeneity of the magnetic field. Our result is $g_I(^{23}Na^+)/g_J(^{23}Na) = [-4.01853 \pm 0.00015] \times 10^{-4}$. Comparing that with a previously measured value of $g_I(^{23}Na)/g_J(^{23}Na) = -4.0184406 \times 10^{-4}$, it affords us no information on the difference in the shielding constants of the atom and ion.

CHAPTER I

INTRODUCTION

"Optical Pumping" has been a very powerful tool in determining nuclear spins, nuclear magnetic moments, and electron magnetic moments since Kastler[1] proposed this method in 1950 and optical pumping has led to valuable experimental and theoretical developments in atomic physics.

In 1958, Dehmelt[2] performed an experiment which achieved the orientation of electrons through spin-exchange collisions with optically pumped Na atoms. This readily opened a door for the study of many more atoms which were difficult to orient directly, because the design, construction, and operation of the resonance lamps would be much more difficult than spin-exchange optical pumping.

Recently Mitchell and Fortson[3,4] reported initial successes with another collisional exchange process, resonant charge-exchange, which can be used to study singly charged ions and neutral atoms having a $^1S_0$ ground-state electronic configuration. In these reports they gave the charge-exchange cross section of Rb and Cs in the temperature range of 20-80°C to be $\sigma_c(Rb^+-Rb) = (7.1 \pm 1.5) \times 10^{-14}\ cm^2$

and $\sigma_c(Cs^+ - Cs) = (8.0 \pm 3.0) \times 10^{-14}$ cm^2 respectively. Oluwole and Togun[5] also gave $\sigma_c(Cs^+-Cs)$ to be

$$(4.5 \pm 0.5) \times 10^{-14} \text{ cm}^2$$

at the temperature of 25°C.

Soon after Mitchell and Fortson's first paper, Nienstadt[6] et. al. also utilized charge-exchange optical pumping to measure the nuclear magnetic moment of free Cs^+ ions.

By the same charge-exchange technique, a precision measurement of $g_I(^{87}Rb^+)/g_J(^{87}Rb)$, measured by Davis, Wright, and Balling,[7] was measured to be -4.969934×10^{-4}. This value with the g factor ratio for the neutral Rb atoms could give rise to the difference of the diamagnetic shielding constants between the atoms and ions. It was this experiment which inspired us to perform the similar experiment with the low Z alkali atoms in order to see the larger difference in the shielding effect of the ions and atoms.

The reasons for choosing Na as a candidate for this experiment is the following:

(1) It is the lowest Z alkali atom next to Hydrogen and Lithium.

(2) It is easier to work with in the experiments than Hydrogen and Lithium. One of the reasons is the wavelengths of the D1 and D2 lines for Hydrogen and

Lithium are very close to each other and can not easily be separated by the standard methods. The wavelengths of the D1 and D2 lines for the alkali atoms are tabulated in Table 1.[8] In addition, Lithium vapor at high temperature produces rapid blackening of all glasses and cracks them when in thermal contact above 200°C.[9] This prohibits the use of a conventional light source and conventional techniques for distilling the Lithium vapor into the sample bulbs.

(3) Na has a nuclear moment of about the same magnitude as Rb which has been successfully charge-exchange optically pumped. The g_I/g_J values, which are related to the nuclear moments, for the Hydrogen-like atoms are listed in Table 2.[10]

In summary, the objectives of this experiment were two-fold. Firstly, to determine the $g_I(^{23}Na^+)/g_J(^{23}Na)$, and then from the known $g_I(^{23}Na)/g_J(^{23}Na)$,[11] derive a difference in the diamagnetic shielding constants between the free Na^+ ions and Na atoms. Secondly, to test the sensitivity of the theoretical S-state wave functions[12,13] by use of the value of the difference in the shielding constants.

The following chapters are a description of the methods used to measure the ratio $g_I(^{23}Na^+)/g_J(^{23}Na)$, and presentation of the results and conclusions of these measurements. Hereafter, we refer to $g_I(^{23}Na^+)/g_J(^{23}Na)$ as g_I^+/g_J. Certain useful preliminary theories, concerning both the experimental method and the diamagnetic shielding effect, are given in Chapter II. The apparatus used in the experiment is presented in Chapter III, and Chapter IV explains the

TABLE 1

D1 and D2 lines for the alkali atoms[8]

	D1(Å)	D2(Å)
H	1215.6738	1215.6684
Li	6709.761	6709.608
Na	5897.5537	5891.5788
K	7701.093	7667.012
Rb	7949.783	7802.406
Cs	8945.952	8523.442

TABLE 2

g_I/g_J values for the hydrogen-like atoms[10]

Element	$g_I/g_J \times 10^{-4}$
H	-15.19270335(14)
D	-2.3321733
T	-1.62051430(17)
Li^6	-2.2356978(10)
Li^7	-5.9042719(10)
Na^{23}	-4.0184406(40)
K^{39}	-0.7088613(6)
K^{41}	-0.3890837(4)
Rb^{85}	-1.4664908(31)
Rb^{87}	-4.96999147(45)
Cs^{133}	-1.9917405(30)

sample preparation. In Chapter V the error analyses and measurement processes associated with the g_I'/g_J are given. Finally, the results, discussion, and conclusions are presented in Chapter VI.

CHAPTER II

THEORY

In this chapter we give an outline of the theory of this experiment. In the first section we will deal with the pumping signals and principles of optical pumping, including the pumping process, relaxation effects, and rf field effect. In order to simplify the equations, we will deal with the case of sodium atoms with zero nuclear spin. The following section will describe the method of charge-exchange optical pumping. The third section will contain the derivation of the Breit-Rabi formula which will be used for the calculation of g_I^+/g_J, and the detailed calculation of g_I^+/g_J is presented in the Appendix A. The final section will describe the calculation of the diamagnetic shielding constant classically and quantum-mechanically.

2.1 OPTICAL PUMPING

1. Brief Description of Optical Pumping of Sodium Atoms

Optical pumping is a process in which light is used to change the relative populations of the atomic energy levels from their normal Maxwell-Boltzmann distribution.

The Zeeman energy splitting between two adjacent substates depends upon the strength of the static magnetic

field. Na has a nuclear spin of I = 3/2 and couples with its ground state, ($^2S_{1/2}$),[14] electronic angular momentum J = 1/2 through the hyperfine interaction to form a resultant total angular momentum F. From the vector model, the possible values of F range from $|I - J|$ to I + J. Each F level has 2F + 1 magnetic sublevels M associated with it. M values range in integral steps from F to -F.[15] Thus Na has a hyperfine doublet and a total of eight substates in the ground state. There are (2,2), (2,1), (2,0), (2,-1), (2,-2), (1,-1), (1,0), (1,1) in the (F,M) representation. The energy level diagram for the relevant atomic states of the sodium in the weak field together with the fine and the hyperfine structures are shown in Fig. 1, and Fig. 2 shows the field-dependent Zeeman splitting of the ground-state of Na atoms.

If a cell containing sodium vapor is placed in an axial, static, magnetic field H_0 along the z axis and illuminated with a left circularly polarized D-1 resonance light incident along the direction of the static field, the following will happen. Some atoms in substates of the ground state will absorb the radiation with the selection rule $\Delta M = +1$, ($\Delta M = -1$ for the right circularly polarized light), and reach the $^2P_{1/2}$ excited state. However, atoms in the (2,2) sublevel of the ground state can not absorb the pumping light since there is no M = 3 sublevel of the $^2P_{1/2}$ state. The atoms pumped to the

Fig. 1 Relevant atomic structure of Na^{23} with I = 3/2 and J = 1/2 energy levels.

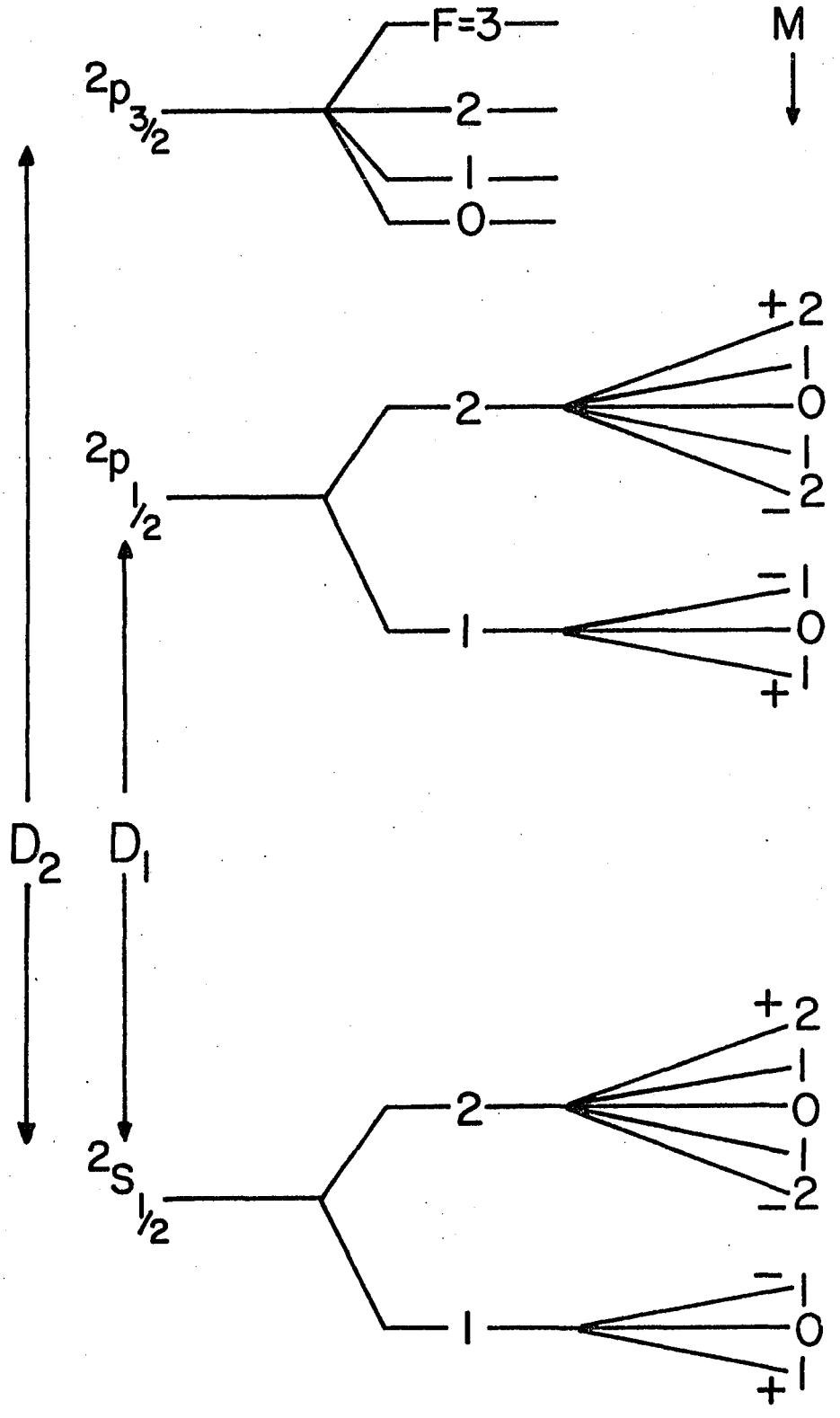

FINE STRUCTURE

HYPERFINE STRUCTURE

ZEEMAN SPLITTING OF HFS IN WEAK MAGNETIC FIELD

Fig. 2 The field-dependent Zeeman splitting of the ground state Na^{23} with I = 3/2.

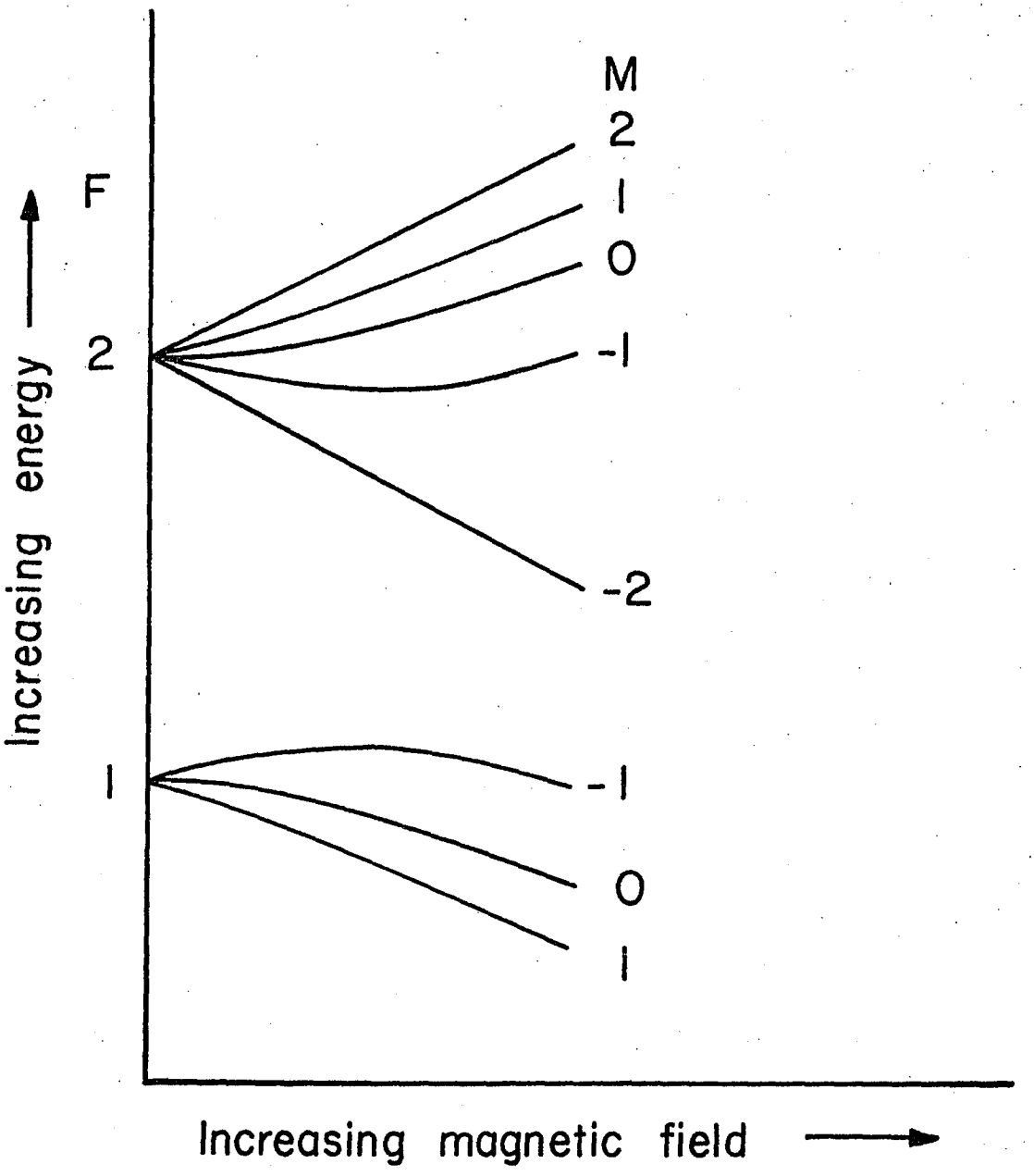
M
2
1
0
-1
-2
F
2
1
-1
0
1
Increasing energy
Increasing magnetic field

$^2P_{1/2}$ will spontaneously decay in about 10^{-8} sec,[16] to some sublevel of the ground state with the selection rule $\Delta M = \pm 1,0$. If we had included the D2 line ($^2S_{1/2} - {}^2P_{3/2}$) in this experiment, the atoms in (2,2) sublevel could absorb light and reach (3,3) sublevel. The D2 would depopulate the substate (2,2) which the D1 has tried to populate. Thus, the pumping is more effective by filtering out the D2 line. Ideally, once the atoms decay to the (2,2) sublevel of the ground state, they remain in this substate indefinitely because the spontaneous decay rate to a lower sublevel is very small.[17] Thus, eventually all the atoms would be pumped to the (2,2) sublevel of the ground state. However, the atoms in (2,2) substate either collide among themselves, buffer gas atoms, or the cell walls, removing atoms from the (2,2) sublevel. As a result, there is a population distribution of the sublevels of the ground state with a larger population in the (2,2) sublevel. An inert gas serves as a buffer gas between the sodium atoms and the cell walls to reduce the effect of wall collisions. The cross sections for disorientation of the ground state sodium atoms caused by the collisions between the inert gas and sodium atoms is very low so the polarization is almost preserved during collisions.[18]

Nevertheless, the polarization produced by the pumping process depends upon the amount of buffer gas pressure

through its effect on the $^2P_{1/2}$ state. If the buffer gas pressure is high enough, a complete mixing in the excited $^2P_{1/2}$ state is expected as the collisional depolarization cross sections of the excited state are relatively large.[19,20] This means that the $^2P_{1/2}$ state sublevels become equally populated before reemission to the ground state. For this situation the probabilities for returning to any ground-state sublevel are all equal.[21]

If we now apply a resonant rf field, which is perpendicular to the static field, to induce transitions between the ground state sublevels, the rf will tend to equalize the populations of the two sublevels, and the number of atoms which can absorb the pumping light will increase. In turn, the intensity of the pumping light transmitted by the optical-pumping cell will drop when the resonant rf field is applied. By monitoring the transmitted light intensity with a photodetector, one can detect the rf transitions.

2. Phenomenological Equations of Zero Nuclear Spin Sodium Atoms.

In order to state the principle of optical pumping and the signal in a simple mathematical form, several assumptions have to be made.

a. Zero nuclear spin of the sodium atoms ($I = 0$)

b. Only D1 ($^2S_{1/2} — ^2P_{1/2}$) and left circularly polarized light is used.

c. A complete reorientation of the excited state

d. No population difference of the sublevels of the ground state at thermal equilibrium.[22]

The energy diagram for a spin-1/2 system for the case of excited state mixing and the pumping cycle is indicated in Figure 3. Consider first the optical pumping of a spin-1/2 system. Let the total number of atoms in the cell be N, and let $N_{\pm}$ denote the number of atoms in the $J_z = \pm 1/2$ sublevels of the ground state. For convenience, we introduce normalized numbers of atoms $n_+ = N_+/N$ and $n_- = N_-/N$, where $N = N_+ + N_-$. Taking assumptions (b), (c), and (d) into consideration, and also the effect of the pumping light upon the sublevels, the rate equations of these two sublevels of the ground state can be written[23]

$$\frac{dn_+}{dt} = \frac{1}{2}\Gamma_p n_- = \frac{n_-}{T_p}$$

$$\frac{dn_-}{dt} = \frac{1}{2}\Gamma_p n_- - \Gamma_p n_- = -\frac{n_-}{T_p}$$

where Γ_p is the probability of an atom in the $J_z = -1/2$ level absorbing a photon. The factor 1/2 reflects the fact that half the atoms raised to the excited state return to the $J_z = -1/2$ level due to complete mixing of the excited state. T_p is the pumping time, and defined as

$$\frac{1}{T_p} \equiv \frac{\Gamma_p}{2} = \frac{1}{2}\int_0^\infty I(\nu)\,\sigma(\nu)\,d\nu \qquad (1)$$

Fig. 3 The optical pumping cycle for a spin-1/2 system with complete collisional mixing in the excited state.

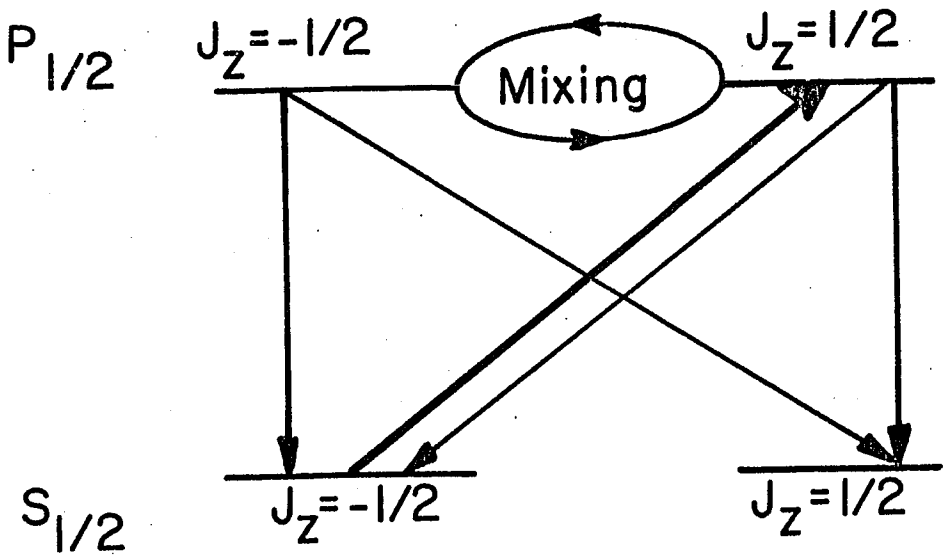
$P_{1/2}$
$J_z=-1/2$
Mixing
$J_z=1/2$
$S_{1/2}$
$J_z=-1/2$
$J_z=1/2$

where $I(\nu)$ is the incident light intensity per unit frequency and $\delta(\nu)$ is the cross section for absorption of a circularly polarized photon of frequency ν. Eventually without any relaxation, the entire ensemble of atoms will be pumped into the +1/2 level.

Now consider the relaxation effects which can result from random collisions between the polarized atoms and the buffer gas atoms or cell walls, and which tend to restore thermal equilibrium and equalize the populations. In the absence of pumping light the return to equilibrium would be exponential with a characteristic time constant T_1 called the longitudinal relaxation time. The rates of change of the population of two levels due to relaxation are written:[24]

$$\frac{dn_-}{dt} = -\frac{1}{T_1}\left(n_- - \frac{1}{2}\right)$$

$$\frac{dn_+}{dt} = -\frac{1}{T_1}\left(n_+ - \frac{1}{2}\right)$$

Here we have made the assumption that all the probabilities for an atom to go from one level to the other level are equal, and each probability is written as $1/2T_1$. Also we have utilized the fact of $1 = n_+ + n_-$.

Next we combine the rate equations for the pumping light and relaxation effects.

$$\frac{dn_-}{dt} = -\frac{1}{T_p}n_- - \frac{1}{T_1}\left(n_- - \frac{1}{2}\right)$$

$$\frac{dn_+}{dt} = \frac{1}{T_p}n_- - \frac{1}{T_1}\left(n_+ - \frac{1}{2}\right)$$

Since we are dealing with the system containing many atoms, we can describe the spin-1/2 system in terms of the ensemble average value of the spin, given by

$$\langle \bar{J}_z \rangle = (+\tfrac{1}{2}) n_+ + (-\tfrac{1}{2}) n_-$$

then the rate equation for $\langle \bar{J}_z \rangle$ becomes

$$\frac{d}{dt}\langle \bar{J}_z \rangle = \frac{1}{2T_p} - \left(\frac{1}{T_p} + \frac{1}{T_1}\right)\langle \bar{J}_z \rangle \tag{2}$$

The equilibrium value of $\langle \bar{J}_z \rangle$ under the influence of pumping and relaxation is obtained by setting $\frac{d}{dt}\langle \bar{J}_z \rangle = 0$

$$\langle \bar{J}_z \rangle_0 = \frac{\frac{1}{2T_p}}{\frac{1}{T_p} + \frac{1}{T_1}} = \frac{T_1}{2T_p} \tag{3}$$

where $1/T_1 = 1/T_p + 1/T_1$

Thus, if there were no relaxation, the atoms would become completely polarized with $\langle \bar{J}_z \rangle_0 = 1/2$. For a given longitudinal relaxation time T_1, the greater the intensity of the pumping light, the closer $\langle \bar{J}_z \rangle_0$ approaches 1/2.

Finally we consider the effects of the rf field. The detection of the signal was accomplished by observing changes in the transmitted light caused by the rf field applied at the resonance frequencies. The principle of this signal detection could be well explained by the classical way of magnetic resonance.[25] What we are interested in is the difference between the values of $\langle \bar{J}_z \rangle$ with and without the rf. The amount of pumping light absorbed will be proportional to N_- or equivalently

to $1 - 2\langle \overline{J}_z \rangle$, assuming the cell is optically thin so that the pumping light intensity will be nearly constant over the length of the cell.

Suppose there is a magnetic field H_0 along the z axis, the equation of motion of the total angular momentum $\vec{J}$ of an atom interacting with the field through its magnetic dipole moment $\vec{\mu}$ is

$$\frac{d}{dt}\vec{J} = \vec{\mu} \times H_0 \hat{K} = \frac{g_J \mu_0 H_0}{\hbar} \vec{J} \times \hat{K} \quad ,$$

where μ_0 is the Bohr magneton and g_J is the g-factor. Since $\frac{d}{dt}\vec{J}$ is orthogonal to $\vec{J}$, the torque produced by the field $H_0\hat{K}$ causes a precession of $\vec{J}$ about the z-axis with angular velocity ω_0. That is $\frac{d\vec{J}}{dt} = \omega_0 \hat{K} \times \vec{J}$, with $\omega_0 = -g_J \mu_0 H_0 / \hbar$.

If we apply an oscillating field with an amplitude $2H_1$ along the x-axis, the resultant magnetic field can be written

$$\vec{H} = H_0 \hat{K} + 2H_1 \cos \omega t \, \hat{i} \quad ,$$

where ω is the oscillation frequency. But

$$2H_1 \cos \omega t \, \hat{i} = (H_1 \cos \omega t \, \hat{i} + H_1 \sin \omega t \, \hat{j}) + (H_1 \cos \omega t \, \hat{i} - H_1 \sin \omega t \, \hat{j}) ,$$

and $\hat{i}$, $\hat{j}$, $\hat{k}$ are the unit vectors along the x, y, and z axes respectively.

That is, the oscillating field is the superposition of two fields rotating in opposite directions as shown in Fig. 4. The component which rotates in the same sense and with nearly the same frequency as ω_0 will exert a torque on $\vec{J}$. The other component could be neglected since it is rapidly changing direction with respect to the direction of $\vec{J}$. The significant part of the magnetic field is

$$\vec{H} = H_0 \hat{K} + (H_1 \cos \omega t \, \hat{i} + H_1 \sin \omega t \, \hat{j}) .$$

In a rotating frame, rotating about the z-axis with the angular velocity ω, the total magnetic field would be

$$\vec{H}' = H_0 \hat{K} + H_1 \hat{i}' ,$$

and the equation of motion for $\vec{J}'$ in the rotating frame is

$$\frac{d\vec{J}'}{dt} = -\omega \hat{K} \times \vec{J}' + \frac{g_J \mu_0 \vec{J}'}{\hbar} \times \vec{H}' = (\omega_0 - \omega) \hat{K} \times \vec{J}' + \omega_1 \hat{i}' \times \vec{J}' ,$$

where $\omega_1 = -\frac{g_J \mu_0 H_1}{\hbar}$

Thus, the equation of motion for the three components of $\vec{J}'$ in the rotating frame are

$$\frac{dJ_x'}{dt} = (\omega - \omega_0) J_y' ,$$

$$\frac{dJ_y'}{dt} = -\omega_1 J_z - (\omega - \omega_0) J_x' ,$$

$$\frac{dJ_z}{dt} = \omega_1 J_y' .$$

Fig. 4 The superposition of two fields rotating in opposite directions.

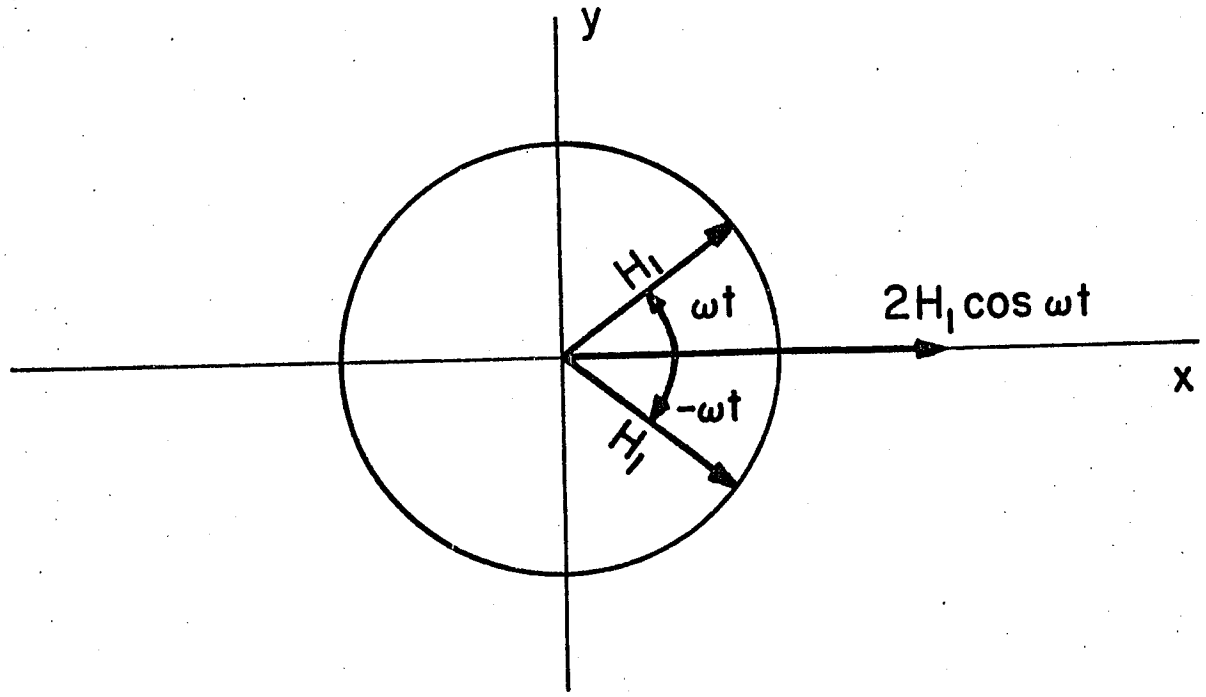
y
H_1
ωt
$2H_1 \cos \omega t$
x
-ωt
H_1

The same basic equations can be derived quantum-mechanically in terms of the expectation value of $\langle \vec{J}' \rangle$.

$$\begin{aligned} \frac{d}{dt}\langle \bar{J}_x' \rangle &= (\omega - \omega_0)\langle \bar{J}_y' \rangle \quad , \\ \frac{d}{dt}\langle \bar{J}_y' \rangle &= -\omega_1 \langle \bar{J}_z \rangle - (\omega - \omega_0)\langle \bar{J}_x' \rangle \quad , \\ \frac{d}{dt}\langle \bar{J}_z \rangle &= \omega_1 \langle \bar{J}_y' \rangle \quad . \end{aligned} \tag{4}$$

The overall equations of motion for $\vec{J}'$, including relaxation, are

$$\begin{aligned} \frac{d}{dt}\langle \bar{J}_x' \rangle &= (\omega - \omega_0)\langle \bar{J}_y' \rangle - \left(\frac{1}{T_p} + \frac{1}{T_2}\right)\langle \bar{J}_x' \rangle \quad , \\ \frac{d}{dt}\langle \bar{J}_y' \rangle &= -(\omega - \omega_0)\langle \bar{J}_x' \rangle - \omega_1 \langle \bar{J}_z \rangle - \left(\frac{1}{T_p} + \frac{1}{T_2}\right)\langle \bar{J}_y' \rangle \quad , \\ \frac{d}{dt}\langle \bar{J}_z \rangle &= \omega_1 \langle \bar{J}_y' \rangle + \frac{1}{2T_p} - \left(\frac{1}{T_p} + \frac{1}{T_1}\right)\langle \bar{J}_z \rangle \quad . \end{aligned} \tag{5}$$

The equilibrium value of $\langle \bar{J}_z \rangle$ with the rf field would be

$$\langle \bar{J}_z \rangle = \frac{\tau_1}{2T_p}\left[1 - \frac{\omega_1^2 \tau_1 \tau_2}{1 + \omega_1^2 \tau_1 \tau_2 + (\omega - \omega_0)^2 \tau_2^2}\right] \tag{6}$$

where $1/\tau_1 = 1/T_p + 1/T_1$; $1/\tau_2 = 1/T_p + 1/T_2$,[26] and T_2 is the transverse relaxation time. Combining equations (3) and (6), the change of $\langle \bar{J}_z \rangle$ due to rf field becomes

$$\langle \bar{J}_z \rangle_\omega - \langle \bar{J}_z \rangle_0 = -\langle \bar{J}_z \rangle_0 \frac{\omega_1^2 \tau_1 \tau_2}{1 + \omega_1^2 \tau_1 \tau_2 + (\omega - \omega_0)^2 \tau_2^2} \tag{7}$$

By the Lambert-Beer law,[27] which states that the amount of radiation ΔI absorbed by an infinitesimally thin layer of absorbing material ΔZ is proportional to

the thickness of the layer and to the intensity I of the radiation incident upon it, that is

$$\Delta I(\nu, z) = -I(\nu, z)\,\sigma(\nu)(n\rho)\,\Delta z$$

where $\sigma(\nu)$ is the cross section for the absorption of light of frequency ν, and ρ is the density of the Na atoms in the cell. Since we assume $I(\nu,z)$ is nearly constant over the length of cell L, i.e. optical thin cell

$$I(\nu, L) = I(\nu,0)\,e^{-\sigma(\nu)(n\rho)L} \simeq I(\nu,0)(1-\sigma(\nu)n\rho L)$$

where $I(\nu,0)$ is the incident light intensity with the light frequency ν

$$I(L) = \int_0^\infty I(\nu,0)\left[1-\sigma(\nu)\rho L\left(\frac{1}{2}-\langle\bar{J}_z\rangle\right)\right]d\nu$$

If we denote the transmitted intensity in the absence of rf as I_0 and the intensity at equilibrium with rf as I_e, then the observed signal

$$\delta I = I_e - I_0 = -\rho L\frac{\gamma_1}{\gamma_p^2}\,\frac{\omega_1^2\tau_1\tau_2}{1+\omega_1^2\tau_1\tau_2+(\omega-\omega_0)^2\tau_2^2}$$

here we have used equations (1) and (7).

This signal has a Lorentzian line shape with central frequency ω_0 and a full-width at half maximum $\Delta\omega = \left(\frac{1}{\tau_2^2}+\frac{\gamma_1}{\gamma_2}\omega_1^2\right)^{1/2}$. The amplitude of the signal is seen to be proportional to the square of the incident light intensity due to the factor of $1/T_p^2$.

2.2 POLARIZATION OF THE NUCLEAR MOMENT OF THE SODIUM IONS BY CHARGE EXCHANGE COLLISIONS

The theory of charge-exchange optical pumping has never been fully worked out. Only a brief description of charge-exchange optical pumping will be presented in this section.

The charge-exchange optical pumping used in this experiment is analogous to spin-exchange optical pumping. Na atoms are oriented by optical pumping. The Na^+ ions produced by a discharge diffuse into the optical pumping region and undergo $Na\text{-}Na^+$ charge-exchange collisions with the oriented neutral Na atoms. The charge-exchange collisions transfer part of the polarization of the neutral atoms to the nuclei of the ions. As a result, the nuclear spins of the ions become polarized. Any change in Na^+ nuclear-spin orientation would partially depolarize the Na atoms through the $Na\text{-}Na^+$ charge-exchange process. Therefore the NMR frequency of Na^+ can be detected by monitoring the transmitted light intensity through the Na sample cell which contained $\sim$ 150 Torr of Ne buffer gas for this experiment.

The nuclear spins are not easily disoriented by collisions with the buffer gas because the Na^+ ions are in a diamagnetic $^1S_0$ ground state. The main relaxation of the nuclear spins is the charge-exchange collisions with the Na atoms. The magnitude of the NMR signals

depends upon the degree of polarization of the neutral Na atoms and the density of the Na atoms in the cell.

2.3 BREIT-RABI FORMULA

The g_I^+/g_J ratio can be calculated from measurements of the Na^+ NMR signal and of Zeeman transitions in Na, using the Breit-Rabi formula.[28-30] The derivation of the Breit-Rabi formula will be presented in what follows.[31]

The Hamiltonian for an atom in a magnetic field H_0 along the z-axis can be written[32]

$$\mathcal{H} = a\,\vec{I}\cdot\vec{J} - g_J\mu_0 H_0 \hat{K}\cdot\vec{J} - g_I\mu_0 H_0 \hat{K}\cdot\vec{I}$$

where a is the dipole interaction constant.

$-g_J\mu_0 H_0 \hat{K}.\vec{J}$ is the interaction energy of the electronic magnetic moment with the magnetic field.

$-g_I\mu_0 H_0 \hat{K}.\vec{I}$ is the interaction energy of the nuclear moment with the magnetic field.

$\vec{I}$ is the nuclear spin.

$\vec{J}$ is the electronic angular momentum.

For convenience, let $b = -g_J\mu_0 H_0$, $c = -g_I\mu_0 H_0$, and use $I_z + J_z = F_z$, the Hamiltonian becomes

$$\mathcal{H} = a\,\vec{I}\cdot\vec{J} + (b-c)J_z + cF_z$$

In order to solve the problem for arbitrary H_0, one must apply degenerate perturbation theory to the $S_{1/2}$ (i.e. J = 1/2) ground state and diagonalize the Hamiltonian in the $|F,M\rangle$ representation.

Since $[F_z, \mathcal{H}] = 0$ in the $|F,M\rangle$ representation, thus

$$\langle F, M | \mathcal{H} | F', M' \rangle = 0 \quad \text{for } M' \neq M \qquad (8)$$ [33]

However, $[F^2, \mathcal{H}] \neq 0$ in the $|F,M\rangle$ representation. This implies there exist off diagonal elements of $\mathcal{H}$ for different F states.

If the wave function of the atom is written as

$$|\psi\rangle = \sum_{F,M} |F,M\rangle\langle F,M|\psi\rangle ,$$

then schrödinger's equation becomes

$$\mathcal{H} \sum_{F,M} |F,M\rangle\langle F,M|\psi\rangle = E \sum_{F,M} |F,M\rangle\langle F,M|\psi\rangle \qquad (9)$$

By taking $\langle F',M'|$ on the left of equation (9) and using equation (8) we have

$$\sum_{F} \langle F', M | \mathcal{H} | F, M \rangle\langle F, M|\psi\rangle = E\langle F', M|\psi\rangle \qquad (10)$$

Since we are considering a S-state atom (J = 1/2), the two values of F for an alkali atom are $F_1 = I + 1/2$, and $F_2 = I - 1/2$, where I = 3/2 for Na. Writing it in matrix form with $|F_{1 \text{ or } 2}\rangle \equiv |F_{1 \text{ or } 2}, M\rangle$, equation (10) becomes

$$\begin{pmatrix} \langle F_1|\mathcal{H}|F_1\rangle & \langle F_1|\mathcal{H}|F_2\rangle \\ \langle F_2|\mathcal{H}|F_1\rangle & \langle F_2|\mathcal{H}|F_2\rangle \end{pmatrix} \begin{pmatrix} \langle F_1|\psi\rangle \\ \langle F_2|\psi\rangle \end{pmatrix} = E \begin{pmatrix} \langle F_1|\psi\rangle \\ \langle F_2|\psi\rangle \end{pmatrix} ,$$

and the energies could be found by solving the secular equation

$$\begin{vmatrix} \langle F_1|\mathcal{H}|F_1\rangle - E & \langle F_1|\mathcal{H}|F_2\rangle \\ \langle F_2|\mathcal{H}|F_1\rangle & \langle F_2|\mathcal{H}|F_2\rangle - E \end{vmatrix} = 0 \quad .$$

Thus the equation becomes

$$E^2 - (\langle F_1|\mathcal{H}|F_1\rangle + \langle F_2|\mathcal{H}|F_2\rangle)E + (\langle F_1|\mathcal{H}|F_1\rangle\langle F_2|\mathcal{H}|F_2\rangle - \langle F_2|\mathcal{H}|F_1\rangle\langle F_1|\mathcal{H}|F_2\rangle) = 0. \quad (41)$$

now the task is to find these matrix elements of the Hamiltonian in this two states system. By using

$$\vec{I}\cdot\vec{J} = \frac{1}{2}(F^2 - I^2 - J^2)$$

$$\langle F|J_z|F\rangle = M\langle F\|\vec{J}\|F\rangle = M\,\frac{J(J+1)-I(I+1)+F(F+1)}{2F(F+1)} \quad ,$$

and $\langle F|J_z|F-1\rangle = \langle F-1|J_z|F\rangle = (F^2-M^2)^{\frac{1}{2}}\langle F\|\vec{J}\|F-1\rangle$

$$= (F^2-M^2)^{\frac{1}{2}}\left[\frac{(F-J+I)(F+J-I)(I+J+1+F)(I+J+1-F)}{4F^2(2F-1)(2F+1)}\right]^{1/2} \quad , \quad 34$$

we have

$$\langle F_1|\mathcal{H}|F_1\rangle = \frac{aI}{2} + \frac{(b-c)M}{2I+1} + cM \quad ,$$

$$\langle F_2|\mathcal{H}|F_2\rangle = -\frac{a(I+1)}{2} - \frac{(b-c)M}{2I+1} + cM \quad ,$$

$$\langle F_1|\mathcal{H}|F_2\rangle = \langle F_2|\mathcal{H}|F_1\rangle = \frac{(b-c)\left[(I+\frac{1}{2})^2 - M^2\right]^{\frac{1}{2}}}{2I+1} \quad .$$

Substituting the above equations into equation (11) and solving for E,

$$E_{\pm} = -\frac{a}{4} + cM \pm \frac{a(2I+1)}{4}\left[1 + \frac{8(b-c)M}{a(2I+1)^2} + \frac{4(b-c)^2}{a^2(2I+1)^2}\right]^{\frac{1}{2}},$$

where the "+" and "-" refer to F_1 and F_2 respectively. Since the hyperfine splitting $\Delta W = \frac{a(2I+1)}{2}$, the above equation can be written in terms of ΔW as

$$E_{\pm} = -\frac{\Delta W}{2(2I+1)} - g_I \mu_0 H_0 M \pm \frac{\Delta W}{2}\left[1 + \frac{4MX}{(2I+1)} + X^2\right]^{\frac{1}{2}}, \quad (12)$$

where $X = \frac{(-g_J + g_I)\mu_0 H_0}{\Delta W}$. Equation (12) is the Breit-Rabi formula.

From the Breit-Rabi formula the NMR frequency $f_2 = -\frac{g_I^+ \mu_0 H_0}{h}$ and the Zeeman transition frequency of (F = 2, M = -1 ↔ F = 2, M = -2), we have

$$\frac{g_I^+}{g_J} = \frac{2Af_2}{\frac{\Delta W}{4h}(1+3A) + f_1(1+A) - \left\{\left[\frac{\Delta W}{4h}(1+3A) + f_1(1+A)\right]^2 - 4Af_1\left(f_1 + \frac{\Delta W}{h}\right)\right\}^{\frac{1}{2}}},$$

or

$$g_I^+/g_J = \frac{f_2(1-A)\left(\frac{\Delta W}{4h} + f_3\right)}{f_3\left(f_3 + \frac{\Delta W}{h}\right)},$$

where $A = g_I/g_J$.

f_1 is the Zeeman transition frequency of (F = 2, M = -1 ↔ F = 2, M = -2).

$f_3 = f_1 + g_I \mu_0 H_0/h$.

The detailed calculation of g_I^+/g_J is given in Appendix A.

The values of g_I/g_J and $\Delta W/h$ for Na used in the calculation of g_I^+/g_J are $-4.0184406 \times 10^{-4}$ [11]

and 1771.6261288 MHz [11] respectively. A computer program for the calculation of g_I^+/g_J is given in Appendix B.

2.4 DIAMAGNETIC SHIELDING EFFECTS

The resonance frequency ν of a nucleus of magnetic moment μ and spin I in a magnetic field H is $\nu = \mu H/Ih$, where h is Planck's constant. H is the magnetic field at the nucleus, which in general is less than the applied magnetic field by a small but important amount which is proportional to the applied field. Thus, one cannot determine the shielding field by merely varying the external field. This difference between the field at the nucleus and the applied field is due to a diamagnetic circulation of the electrons produced by application of the external field. The effect of the diamagnetic shielding was first estimated from a classical theory by Lamb[35] for nuclei of atoms with spherically symmetrical nuclear electric potentials. This type of calculation is quite good for atoms and for heavy atoms in molecules, since in the latter case most of the shielding comes from the innermost electrons. However, the precision of recent experiments has become so great that Lamb's correction is no longer good enough. Ramsey[36-39] has developed a more general correction of diamagnetic shielding, consisting of two parts: (1) a

relatively simple term corresponding to Lamb's correction, and (2) a complicated term arising from second-order paramagnetism. This second term physically comes from the fact that the presence of the attracting centers from several different massive nuclei prevents a simple circular diamagnetic circulation of the electrons about any one nucleus. In other words, the second term corrects the shielding effect because of the fact that the nonspherical symmetrical nuclear electric potentials due to the presence of the other nuclei in the same molecule. Fortunately in this experiment, since we are dealing with the Na atom, only the first term is to be considered. The theory of the diamagnetic shielding for nuclei of atoms will be presented in the following

1. Classical Approach

Lamb's[35] original calculation of the shielding constant was somewhat tedious. We follow Dickinson[13] and Armstrong's[40] approach.

Consider an atom with a spherically symmetrical charge distribution of radial density $\rho(r)$ in an external field H. The amount of charge contained in a volume element taken as a ring with axis passing through the nucleus and parallel to the external field H is

$$\rho(r)\, 2\pi r^2 \sin\theta \, d\theta \, dr$$

but the total charge density $\rho(\vec{r})$ relates to the radial density $\rho(r)$ as $\rho(\vec{r}) = 4\pi r^2 \rho(r)$. Thus the total charge contained in a volume element becomes

$$\frac{\rho(\vec{r})}{2} \sin\theta \, d\theta \, d\gamma$$

The current arises from the rotation of this charge ring with the Larmor frequency $\frac{eH}{4\pi mc}$ is

$$di = \left[\frac{\rho(\vec{r})}{2} \sin\theta \, d\theta \, d\gamma\right] \frac{eH}{4\pi mc} \quad . \tag{13}$$

Hence by the Biot-Savart law the induced field dH'(0) at the nucleus due to this current loop is

$$dH'(0) = \frac{2\pi \sin^2\theta \, di}{\gamma c} \quad . \tag{14}$$

Substituting equation (13) into equation (14) and integrating over angles, the ratio of induced field to the external field is

$$\frac{H'(0)}{H} = \frac{e}{4mc^2} \int_0^{\pi} \sin^3\theta \, d\theta \int_0^{\infty} \frac{\rho(\vec{r})}{\gamma} d\gamma = \frac{e}{3mc^2} V(0) \, , \tag{15}$$

where v(0) is the potential at the nucleus due to the atomic electrons. This potential is negative; the induced field is opposed to the external field. This effect is known as diamagnetic shielding and the ratio of induced field to the external field is called the diamagnetic shielding constant σ, which can also be written in terms of the fine structure

constant $\alpha = \frac{e^2}{\hbar c} = \frac{1}{137}$, Bohr radius $a_0 = \frac{\hbar^2}{me^2} = 0.5292\text{Å}$ and $v(0) = -Ze(1/r)_{Av.}$ Equation (15) becomes

$$\sigma = \frac{Z}{3}\alpha^2 \left\langle \frac{1}{r} \right\rangle_{AV.} \quad , \tag{16}$$

where Z is the atomic number and $\langle r \rangle_{Av.}$ is the average distance of the electron from the nucleus in Bohr radii. For a more accurate determination of v(0), we can consider the Thomas-Fermi model of the atom[41-45] in which the total electrostatic potential at a distance from the nucleus r = bx is

$$V(r) = \left(\frac{Ze}{bx}\right)\phi(x) \quad ,$$

where $\phi(x) = 1 - 1.588x + (4/3)x^{3/2} + \ldots$ [46] for small x, and $b = 0.885\, a_0/Z^{1/3}$. Then the electronic contribution to the potential at the nucleus is $v(0) = -1.588 \frac{Z^{1/3} e}{0.885\, a_0}$ Substituting into equation (15), it becomes

$$\sigma = 0.319 \times 10^{-4} Z^{4/3}$$

2. Quantum-Mechanical Approach

Assume that the nuclei can be treated classically as stationary attracting centers. This essentially means that no energy terms corresponding to nuclear motion appear in the Hamiltonian. The general method of attack is to develop an expression for the interaction energy of the nucleus and the external magnetic field. We assume that we can write the interaction energy as the sum of two terms

$$W = -\vec{\mu}\cdot\vec{H} = -\vec{\mu}\cdot\vec{H}_0\,[1-\sigma_\lambda] = W_\lambda^{(0)} + W_\lambda$$

where σ_λ is the desired shielding constant $W_\lambda = \vec{\mu}\cdot\sigma_\lambda\vec{H}_0$ is the interaction energy of the nuclear magnetic moment with the magnetic field produced by the electronic motion resulting from the applied field, and λ represents the nuclear orientation. Using perturbation theory, we now calculate the perturbed energy of the electron system and use all the terms linear in μ and H as W_λ . The notation used is:

$\vec{\mu}$ nuclear magnetic moment

$\vec{H}_0$ applied external magnetic field

$\vec{A}$ net vector potential from the applied field plus the nuclear moment

-e electronic charge

V electrostatic potential energy function for the electrons

$\vec{P}$ electron momentum

The Hamiltonian of the electron system is

$$\mathcal{H} = \sum_K \frac{1}{2m_K}\left(\vec{P}_K + \frac{e}{c}\vec{A}_K\right)^2 + V$$

or

$$\mathcal{H} = \sum_K \frac{1}{2m_K}\left[\left(P_{xK}+\frac{e}{c}A_{xK}\right)^2 + \left(P_{yK}+\frac{e}{c}A_{yK}\right)^2 + \left(P_{zK}+\frac{e}{c}A_{zK}\right)^2\right] + V \,, \qquad (17)$$

where $A_K = \frac{1}{2}\vec{H}_0 \times \vec{\gamma} + \frac{\vec{\mu}\times\vec{\gamma}}{\gamma^3}$ [47], the first term arises from the uniform applied field $\vec{H}_0$, and the second term comes from the nuclear magnetic moment $\vec{\mu}$. If we make the z-axis parallel to the applied field and $\vec{\mu}$, the three components of $\vec{A}$ become

$$A_x = -\frac{1}{2}H_0 y - \frac{\mu y}{r^3}$$

$$A_y = \frac{1}{2}H_0 x + \frac{\mu x}{r^3} \qquad (18)$$

$$A_z = 0 \ .$$

Replacing p_{xk} by $\frac{\hbar}{i}\frac{\partial}{\partial x_K}$ etc. in (17) and using (18) we obtain

$$\mathcal{H} = -\sum_K \frac{\hbar^2}{2m_K}\nabla_K^2 + V + \left\{-\sum_K \left(H_0 + \frac{2\mu}{r_K^3}\right) m_{zK}^0 + \frac{e^2}{8mc^2}\sum_K \left(H_0 + \frac{2\mu}{r_K^3}\right)^2 (x_K^2 + y_K^2)\right\} .$$

Let

$$\mathcal{H} = \mathcal{H}_0 + \mathcal{H}'$$

$$\mathcal{H}_0 = -\sum_K \frac{\hbar^2}{2m_K}\nabla_K^2 + V$$

$$\mathcal{H}' = \left\{-\sum_K \left(H_0 + \frac{2\mu}{r_K^3}\right) m_{zK}^0 + \frac{e^2}{8mc^2}\sum_K \left(H_0 + \frac{2\mu}{r_K^3}\right)^2 (x_K^2 + y_K^2)\right\} , \qquad (19)$$

where

$$m_{zk}^0 = -\frac{e\hbar}{2mci}\left(x_K\frac{\partial}{\partial y_K} - y_K\frac{\partial}{\partial x_K}\right) .$$

Now we treat the H' as a perturbation and calculate the perturbed energy level only to first order because we are dealing with the simple atomic case. The first order correction term to the unperturbed energy is

$$W_1 = \langle \Phi | \mathcal{H}' | \Phi \rangle$$

Since we are interested in the term linear with H_0, thus from inspection of equation (19), the part of W_1 linear with μH_0 is

$$\frac{e^2 \mu H_0}{2mc^2} \sum_K \langle \Phi \lambda \left| \frac{x_K^2 + y_K^2}{r_K^3} \right| \Phi \lambda \rangle \quad .$$

Therefore, the shielding constant with nuclear orientation specified by λ is

$$\sigma_\lambda = \frac{W_\lambda}{\mu H_0} = \frac{e^2}{2mc^2} \langle \Phi \lambda \left| \sum_K \frac{x_K^2 + y_K^2}{r_K^3} \right| \Phi \lambda \rangle$$

Remembering that λ specifies the nuclear orientations, it must be averaged over all orientations. In such an average, the x, y, and z coordinates must all be equivalent. Thus, one has the shielding constant

$$\sigma = \frac{e^2}{3mc^2} \langle \Phi \left| \sum_K \frac{1}{r_K} \right| \Phi \rangle = \frac{\alpha^2}{3} \langle \Phi \left| \sum_K \frac{1}{r_K} \right| \Phi \rangle \qquad (20)$$

where again α is the fine structure constant and r_k is the distance of the kth electron from the nucleus in Bohr radius, with the summation extending over all the electrons in the system. Equation (20) is the same as equation (16) except equation (16) was written in terms of the average distance for all the Z electrons in the system.

Based on equation (20), Dickinson[13] evaluated σ for the atomic number Z in the range $1 \leq Z \leq 92$ using Hartree and Hartree-Fock wavefunctions,[48,49] and Kopfermann[50] evaluated $K = (1 + \sigma)^{-1}$ in the same range using Hartree wavefunctions. Bonham and Strand[51] have evaluated σ by employing Hartree-Fock charge densities for small Z and Thomas-Fermi-Dirac densities for large Z. Malli and Fraga[52] have calculated σ using Hartree-Fock wave functions for ground and excited

states of neutral atoms and positive and negative ions. The theoretical values of σ for Na and Na^+ from the work mentioned above will be discussed in a later chapter.

CHAPTER III

APPARATUS

Sodium resonance radiation is circularly polarized and passed through an optical pumping cell containing the sodium vapor and Ne buffer gas. The sodium atoms in the cell are oriented in a magnetic field through the absorption and the reemission of the pumping light. When a rf field, perpendicular to the static field, is applied at either the Zeeman frequency or NMR frequency, the sodium atoms become depolarized, resulting in a decrease in the intensity of the transmitted pumping light which is detected by a photocell. Much of the equipment used was similar to previous work.[7] A block diagram of the apparatus is shown in Fig. 5.

3.1 SODIUM LIGHT SOURCE AND ACCESSORIES

A sodium light source is difficult to build, since sodium vapor reacts strongly with Pyrex at 200°C or greater. The walls turn brown, and sometimes the reaction even cracks the Pyrex. It is not acceptable to have a sodium light source with a dark wall because sodium D lines lie in the visible spectral range. The opaqueness would severely attenuate the intensity of the pumping light.

The light source used herein was a dc discharge lamp. The bulbs used were commercial G.E. Na-1 sodium light bulbs.[54]

Fig. 5 Block diagram of the apparatus.

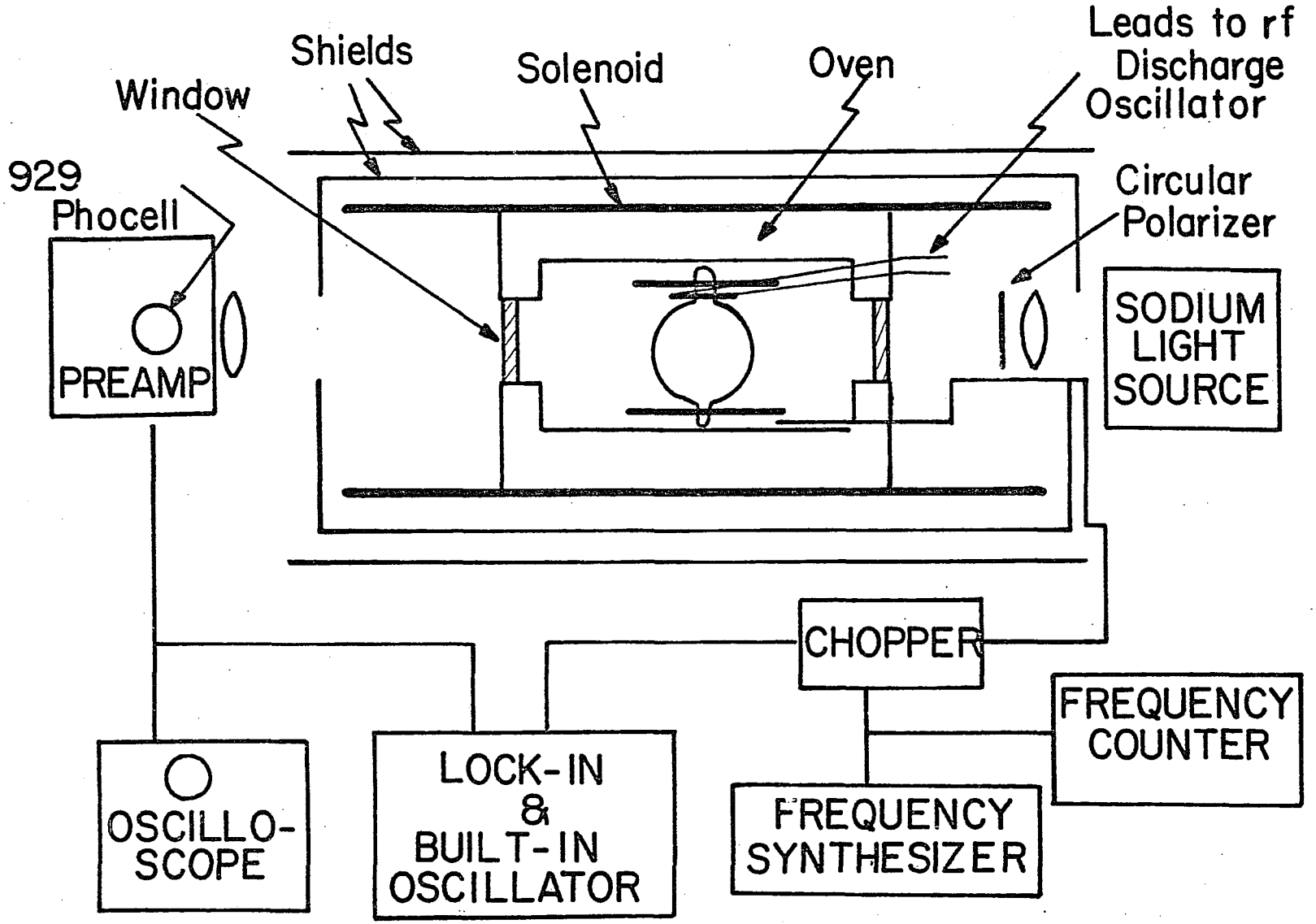
Leads to rf
Discharge
Oscillator
Shields
Solenoid
Oven
Window
929
Phocell
Circular
Polarizer
PREAMP
SODIUM
LIGHT
SOURCE
CHOPPER
FREQUENCY
COUNTER
OSCILLO-
SCOPE
LOCK-IN
&
BUILT-IN
OSCILLATOR
FREQUENCY
SYNTHESIZER

The bulb was surrounded by an oven with a $\sim 5\Omega$ conical heater powered by dc power supply to get rid of the possibility of 60 cycle noise. The construction of this oven has been described in detail by Davis.[55] The Na light bulb with the oven is shown in Fig. 6. The Na light bulb was powered by an adjustable current-regulated dc supply. Most of the time, the light had a stable emission when the current ran at ~ 3.7 Amp. The schematic diagram of the current-regulated dc power supply for the light source is shown in Figure 7.

The light passes through a linear polaroid, a quarter wave plate, and a four inch diameter convex lens. The linear polaroid and quarter wave plate have to be arranged so that the light passing through is circularly polarized. The circularly polarized light can be produced by orienting the axis of the quarter wave plate at an angle of 45^{o} with the axis of the polaroid.[56] For convenience, the quarter wave plate was set so that it could be rotated to produce left circularly, right circularly, or linearly polarized light.

An interference filter[57] was not used due to the fact that the sodium D lines are too close together to be separated (cf., Table 1). Technically it is very difficult to make a filter which has a wave band-width less than $6\mathring{A}$. However, the pumping cycle becomes much more efficient if only D1 light is used. The D2 resonance intensity normally could be decreased through the process of self-reversal.[58,59]

Fig. 6 Sodium light source with its oven.

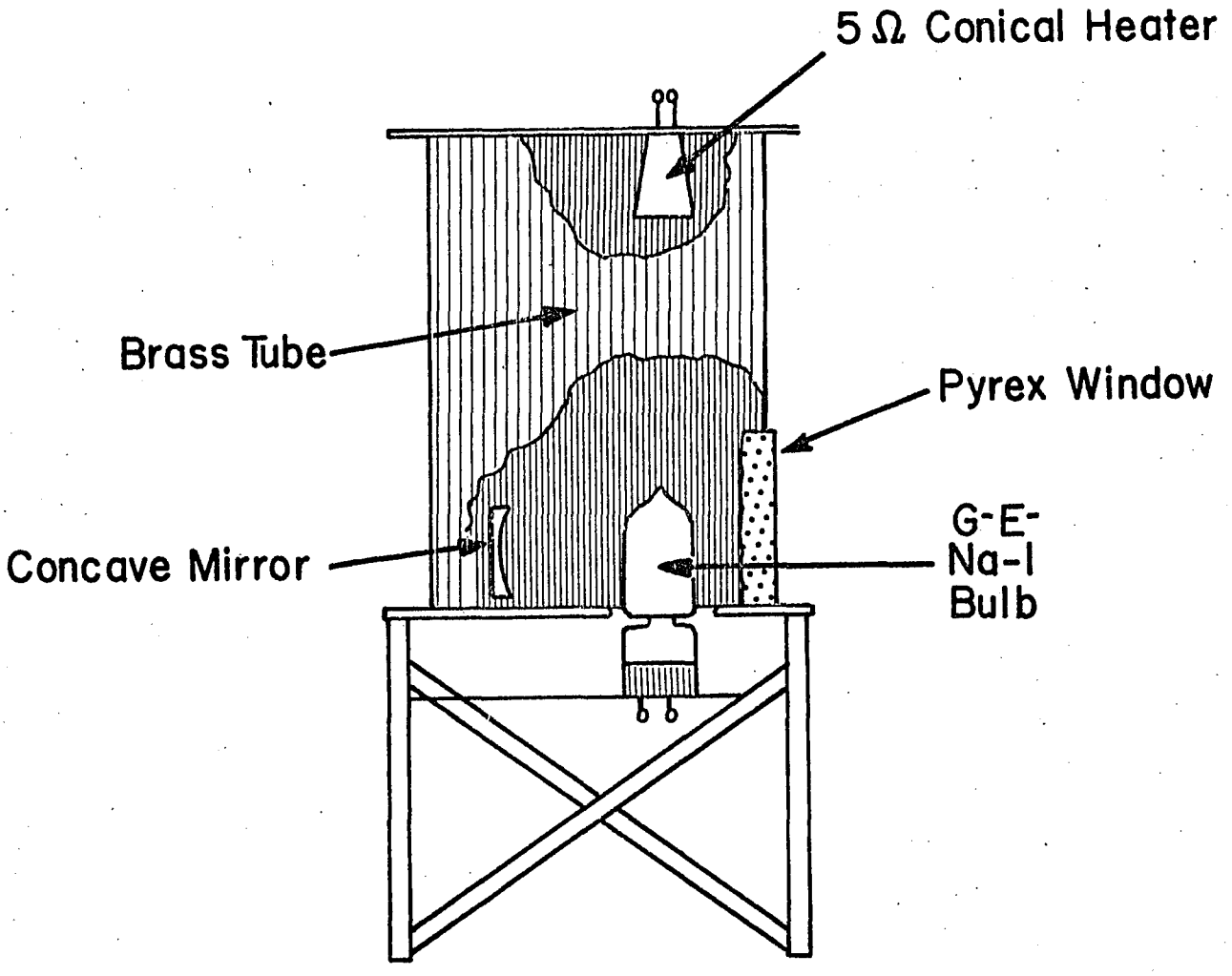
5 Ω Conical Heater
Brass Tube
Pyrex Window
Concave Mirror
G-E-
Na-I
Bulb

Fig. 7 A schematic diagram of the current-regulated power supply for the sodium light source.

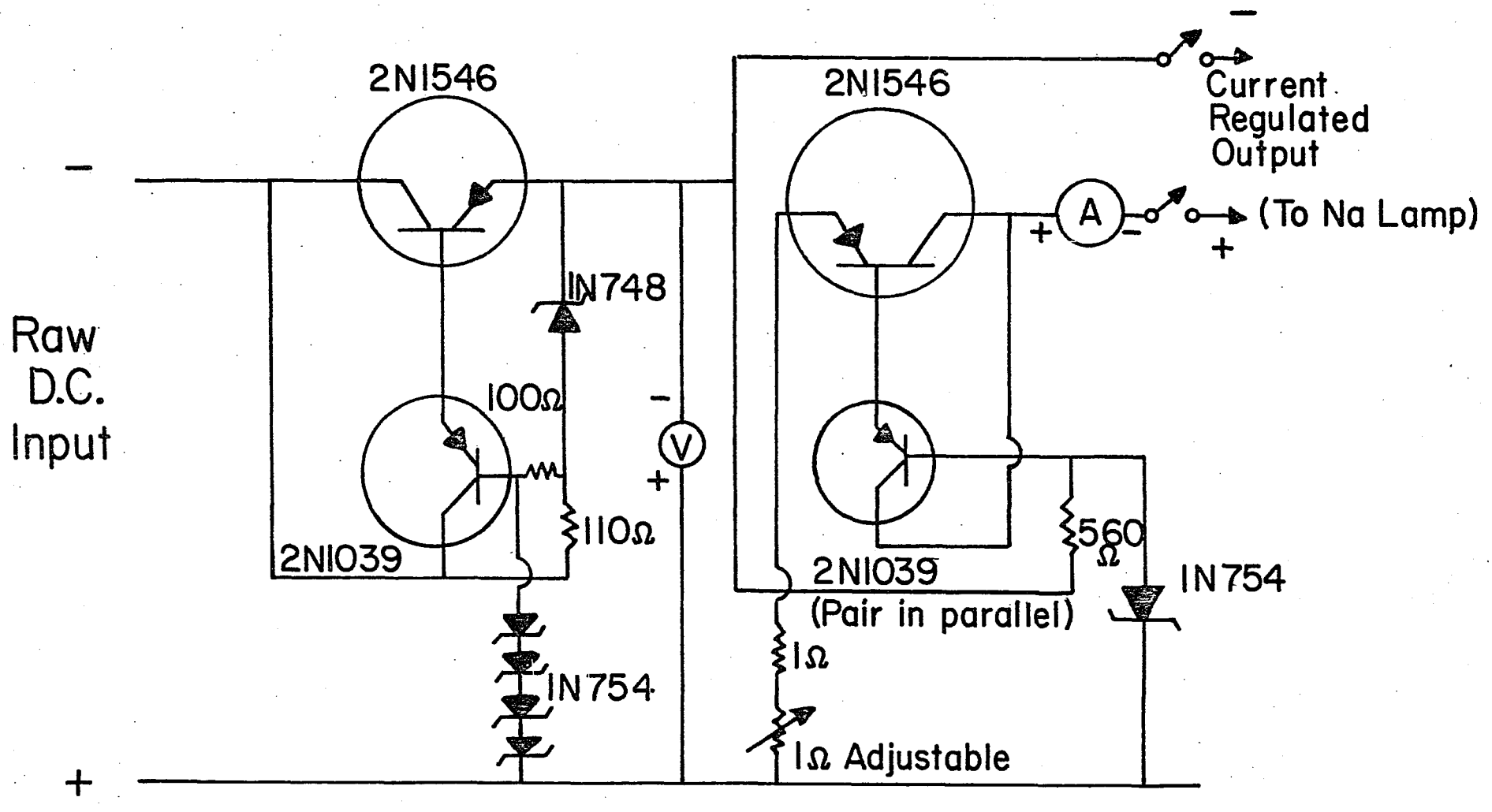
2N1546
2N1546
Current
Regulated
Output
(To Na Lamp)
A
IN748
100Ω
Raw
D.C.
Input
V
110Ω
2N1039
560
Ω
2N1039
(Pair in parallel)
IN754
IN754
1Ω
1Ω Adjustable

The usual case for self-reversal in a lamp occurs because the vapor in the central part of the lamp, where the discharge occurs, is hotter than the cooler outer regions. If there is sufficient vapor in these outer region, it will absorb some of the resonance light coming from the central portion of the lamp. The resonance light of course contain two D lines, however, the D2 line has more absorption than D1 because D2 line involves a greater number of possible transitions.[60] Hence the net effect of the ratio of D1(intensity)/D2(intensity) increases.

Since self-reversal is a temperature dependent process, the temperature of the lamp could be adjusted by varying the conical heater current. The voltage applied to the heater was recorded when the optical pumping signal was maximum. The lamp was run near or at this voltage for the entire experiment.

A holder containing the convex lens, and circular polarizer was situated inside the solenoid so that the light source could be moved close to the end plate of the cylindrical shield to maximize the light intensity.

3.2 MAGNETIC FIELD

This section contains the description of (1) the shielded solenoid with second order correction coils, (2) the ultra-stable regulated power supply which

supplied the power to the solenoid, (3) the Helmholtz coils which produced the rf field.

1. Shielded Solenoid with Second Order Correction Coils

Measurements require a narrow line-width of both the Zeeman and NMR signals. The Zeeman line-width broadening is mainly due to the inhomogeneity of the magnetic field. Therefore a stable and homogeneous magnetic field is necessary. We used a shielded solenoid which was similar to the system described by Hanson and Pipkin.[61] The solenoid had a 36 inch length and a 12 inch diameter, and was surrounded by three concentric cylindrical Mollypermalloy shields. The shields were equipped with demagnetization coils which allowed the experimenter to produce strong A.C. fields in various directions within the shields themselves. After a large change in the field of the solenoid had been made, a 60 Hz current was passed through the demagnetizing coils and slowly decreased to zero. This process was necessary to avoid large inhomogeneities due to magnetization of the shields themselves.[62] The shields were also furnished with removable end caps with three inch diameter holes cut in the center. A second order correction coil was used to improve the axial homogeneity of the field. This coil is designed to cancel the second order functional dependence of the field upon z, the distance from the center of the solenoid along the axis. The magnetic field produced by the solenoid can

be expanded in a power series in z, with all odd power vanishing because of symmerty. Due to the need of an oven inside the solenoid for heating the Na in the sample cell, and the heat produced by the current through the solenoid itself, a copper tubing with 0.281 inch o.d. was wound around the outside so the solenoid could be water cooled. A 10 inch diameter and 10 inch long aluminum cylinder, which fit inside the solenoid, was used as a housing for the oven. A thin layer of fiberfrax wrapped around inside and outside of the aluminum cylinder served as an insulator between the cylinder and the solenoid. Two 10-inch diameter wooden caps with a 4-inch diameter window in the center were used to form an enclosed oven. The temperature of the inside of the oven was measured with copper-constantan thermocouples sticking in the oven through a wood cap.

2. Ultra-stable Regulated Power Supply

The solenoid was powered by a current regulated supply which had a short-term stability of 10^{-7}. Only 2.45 Ampere, and 2.85 Ampere were separately used in this experiment. However, 2.85 Ampere which produced a magnetic field of ~57 Gauss, was used for the most of the runs.

A 1 Henry choke and two 3000 MFD capacitors with 150 VDC were connected as a low pass filter to this

power supply. The schematic diagram of this supply is shown in Figure 8. The magnitude of the regulated current could be varied by changing the voltage of a battery. In this experiment, for example, the voltages used were 7.5 Volts and 6.9 Volts for the current of 2.85 Ampere and 2.45 Ampere respectively.

3. Helmholtz Coils

Two pairs of Helmholtz coils were used alternatively for the measurements of the NMR frequency and the Zeeman transition frequency. A pair of Helmholtz coils was made out of one turn copper wires with the diameter as large as possible ($\sim$18 cm) in order to minimize asymmetries in the Zeeman line shape due to a combination of the inhomogeneities in the rf and static fields.[63] Another pair of six-turn Helmholtz coils made with the diameter $\sim$ 20 cm was used for measuring NMR frequency. A power amplifier, (1233-A model made by General Radio Company), was used to amplify the NMR signal because the nuclear moments are much smaller than the electronic magnetic moments. In order to prevent overloading the power amplifier, we put a 50 Ω resistor in series with the six-turn coil. A switch was built to bypass the power amplifier and 50 Ω resistor when the measurements of the Zeeman frequency were made by the use of the one-turn Helmholtz coil.

Fig. 8 A schematic diagram of the ultra-stable power supply for the static magnetic field.

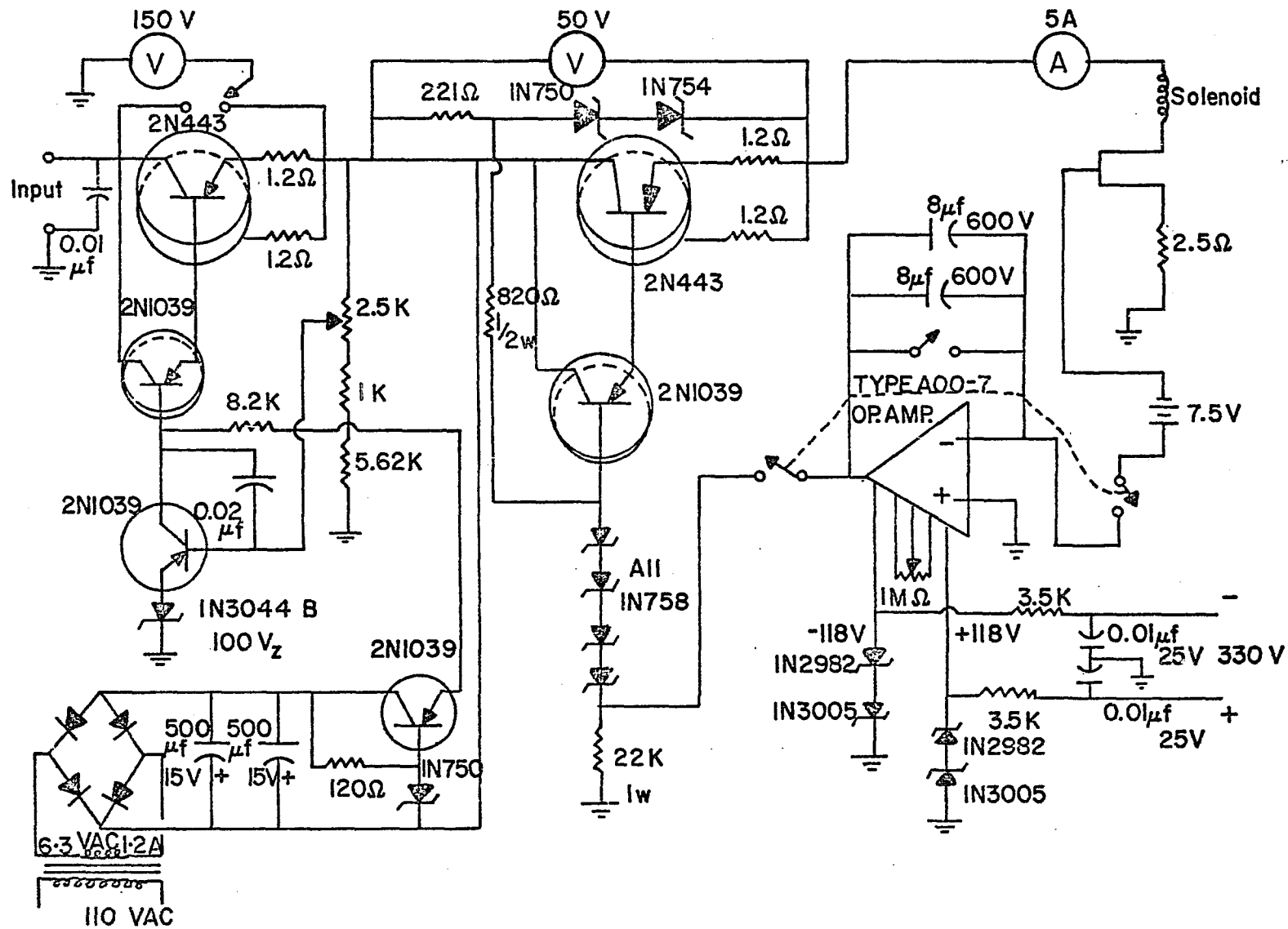
150 V
V
2N443
Input
0.01 μf
1.2Ω
1.2Ω
2N1039
2.5 K
1 K
8.2K
5.62K
2N1039
0.02 μf
IN3044 B
100 Vz
2N1039
500 μf 15V +
500 μf 15V +
120Ω
IN750
6·3 VAC 1·2A
110 VAC
50 V
V
221Ω
IN750
IN754
1.2Ω
1.2Ω
2N443
820Ω ½w
2N1039
A11
IN758
22K
1w
5A
A
Solenoid
2.5Ω
8μf 600 V
8μf 600V
TYPE A00-7
OP. AMP.
7.5V
1MΩ
3.5K
-118V
IN2982
IN3005
+118V
0.01μf 25V
330 V
3.5K
IN2982
IN3005
0.01μf 25V
+
-

3.3 SIGNAL DETECTION DEVICE

The detection of the Zeeman signals or NMR signals were accomplished by observing the changes in the transmitted pumping light caused by the rf field applied at either the Zeeman frequencies or the NMR frequency. The rf depolarized the oriented Na atoms at either the Zeeman frequencies or the NMR frequency resulting in a decrease of the transmitted light. This is the principle of the detection technique.

The rf produced by the frequency synthesizer (1164-A type; 0.01-70 MHz) fed into both a Hewlett-packard 5254L frequency counter and into a pair of Hewlett-packard rf attenuators which allowed attenuation of the rf from 0-132 db in integral steps. This output voltage was coupled into a chopper which chopped the rf with a rate of 11 Hz. The frequency of the chopper was determined by the frequency of a reference signal put out by the Princeton Applied Research model HR-8 Lock-in Amplifier. Therefore the rf was square wave modulated at a rate of 11 Hz. This meant that the transmitted light intensity was also modulated at 11 Hz since the bulb absorbs some pumping light while the rf is on and becomes more transparent in the absence of rf. The modulated transmitted light was detected by a #929 photocell.[64] The photocell circuit is shown in Figure 9. The A.C. output was amplified by a Tektronix 122 preamplifier before display on a Tektronix 504 oscilloscope and P.A.R. Lock-in Amplifier. The oscilloscope allowed the visual observation of the signal, while the

Lock-in amplifier allowed the detection of the smaller signals.

Fig. 9 Photocell circuit diagram.

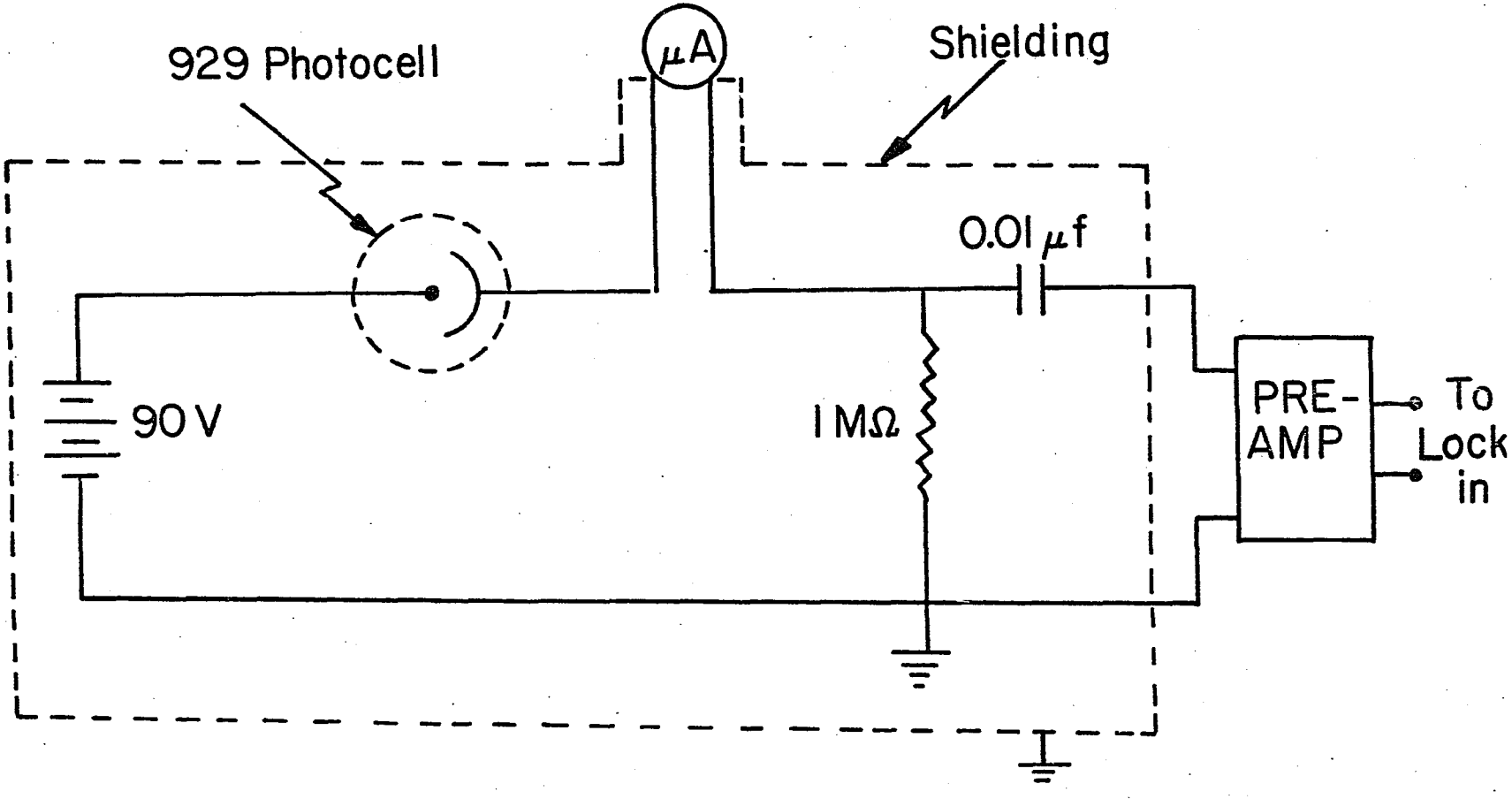
929 Photocell
μA
Shielding
0.01 μf
90 V
1 MΩ
PRE-
AMP
To
Lock
in

CHAPTER IV

SAMPLE PREPARATION

Two types of cells were specifically purchased from the glass-blower.[65] One is the 300 cm^3 pyrex spherical bulb, while the other is 1.25 inch radius and 1.5 inch long pyrex cylindrical bulb. All the cells had a one inch long 6 mm o.d. stem on the bottom to serve as a reservoir for the sodium metal, and also had a pair of turrets on the top. The discharge for the production of Na^+ ions was run between glass-covered electrodes in the turret. The gap between two electrodes was $\sim$2 cm. The geometrical shape of the bulbs are shown in Figure 10. The electrodes were powered by a rf oscillator to ionize the sodium vapor. The Na^+ ions diffused to the pumping region where the charge-exchange process took place.

An one gram with 99.95 % purity sodium ampoule[66] was put into a 1.5 cm o.d. glass tube which was blown onto the sample cell which was then attached to the oil diffusion pump vacuum system. All the cells and glass tubing were cleaned with a 5 % Hydro-fluoric acid solution and rinsed six times with distilled water and then allowed to dry before they were attached to the vacuum system.

When the sample was pumped down to 10^{-6} Torr we baked the cell and maintained the temperature of 500^{o}C for two

Fig. 10 Two types of sample cells: (i) 300 cc spherical flask (ii) 150 cc cylindrical bulb.

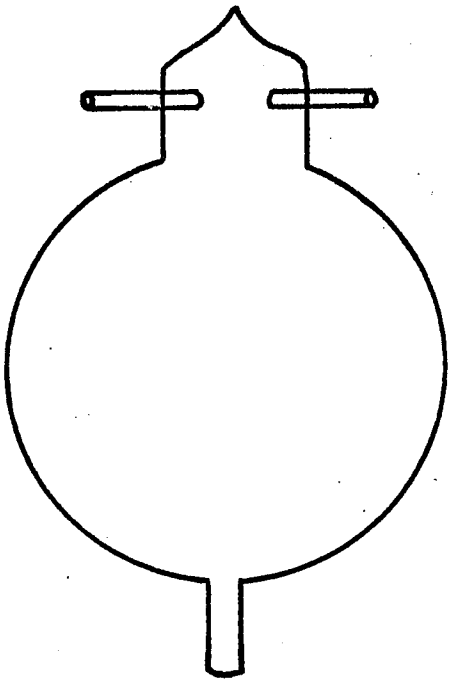

(i)

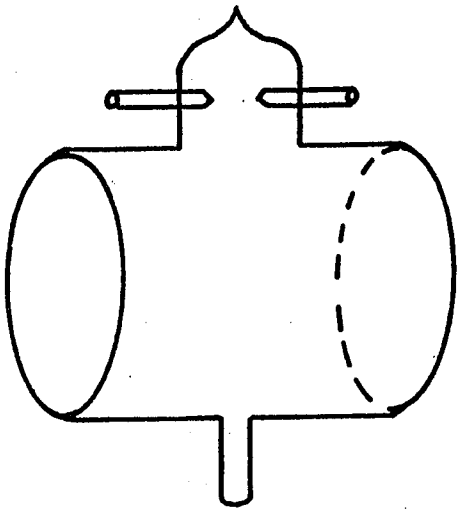

(ii)

hours. We then drove the sodium into the cell when the pressure of the sample system was about 5×10^{-6} Torr. Sodium tends to react with glass to make it brown, and therefore opaque. It was found that by distilling only a small amount of sodium at a time, forming a fine film on the cell, that the sodium could be driven into the bulb tip or lower part of the bulb without blackening the cell. This distillation process was then repeated several times to assure that there was an adequate supply of sodium for the experiment.

Once there was enough sodium in the bulb, we immediately sealed off the glass tube, and pumped the bulb pressure down to 5×10^{-6} Torr. Once this bulb pressure was reached, we put ~150 Torr of Neon buffer gas[67] into the bulb. Buffer gas pressure measurements were made with an oil manometer.

The entire process of sample preparation is shown in Figure 11. All the measurements we report here were made with the 300 cm^3 spherical sample bulb to take advantage of the larger signal in the bigger bulb.

Fig. 11 Outline of the process for the sample preparation.

① Sample at beginning of pump down

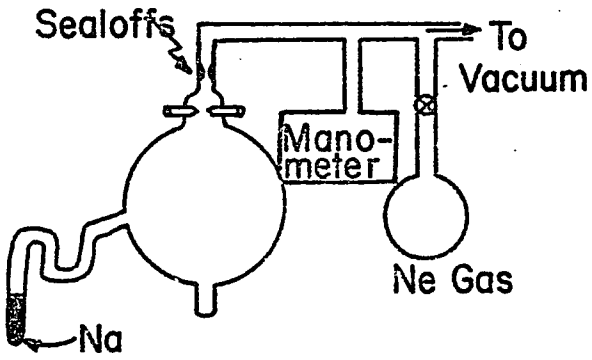

② Drive Na in the bulb

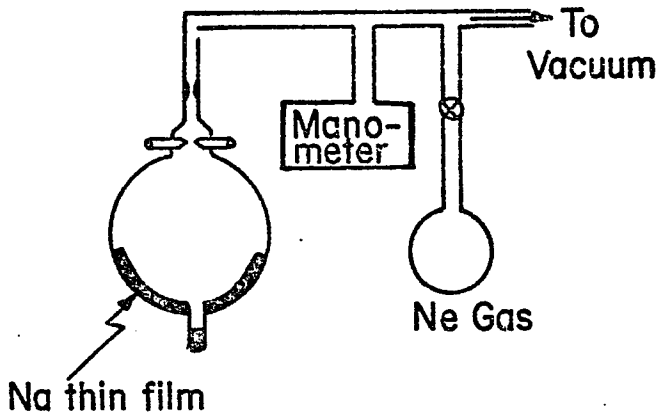

③ Finished sample with ~150 Torr Ne

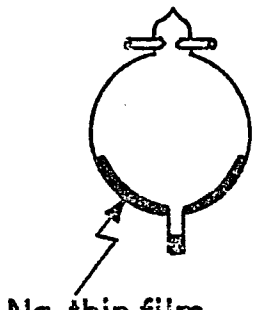

CHAPTER V

MEASUREMENTS AND ERROR ANALYSIS

This chapter deals with the measurement procedures and error analysis. What we are interested in here is the nuclear magnetic resonance frequencies of sodium ions and Zeeman transition frequencies of sodium atoms. All these measurements of frequencies were measured with a digital frequency counter with an accuracy of $\pm$ 1.0 Hz.

5.1 OBSERVATIONAL MEASUREMENTS

g_I^+/g_J can be calculated with the aid of the Breit-Rabi formula (see Appendix A) from the NMR frequency and the Zeeman transition frequency ($F = 2, M = -1 \leftrightarrow F = 2, M = -2$).

The apparatus was turned on for at least two hours before making the measurements. It was found that the ultra-stable power supply, which supplied the current through the solenoid, would operate better after two hours of continuous operation. An effort was also made to shim the magnetic fields prior to each run since the inhomogeneity of magnetic fields would broaden the line-width of Zeeman frequencies. The line-width could be greatly reduced by adjusting the current through the second order correction coil and the position of the end plates. The best optical

pumping signals were obtained with a sodium atom vapor pressure of $\sim 10^{-5}$ Torr. Figure 12 shows the vapor pressure of the sodium as a function of temperature.[68] The sodium vapor pressure is 10^{-5} Torr at 150^{o}C. Two pieces of fire bricks were used as the base for the Helmholtz coils and the heater, which was powered by a variac. The variac was turned off while making a series of measurements and was turned back on when the signals became weaker. This series of measurements generally consisted of four determinations of the NMR frequency and five determinations of the Zeeman frequency. Each determination of the NMR frequency consisted of four NMR peak frequency measurements. Each determination of the Zeeman frequency was the average of three measurements of the frequency of the Zeeman signal peak. The variac was turned on and off throughout the entire run until we had made roughly twenty determinations of NMR frequency and twenty one determinations of Zeeman frequency.

Each measurement of g_I^+/g_J was based on one determination of the NMR frequency and an average value of two determinations of the Zeeman frequency to compensate for field drift. There were approximately twenty g-factor ratio measurements for every run except for a couple of runs which contained more than twenty g-factor ratios. All the measurements were done with the right circular

Fig. 12 The vapor pressure of the Na as a function of temperature.

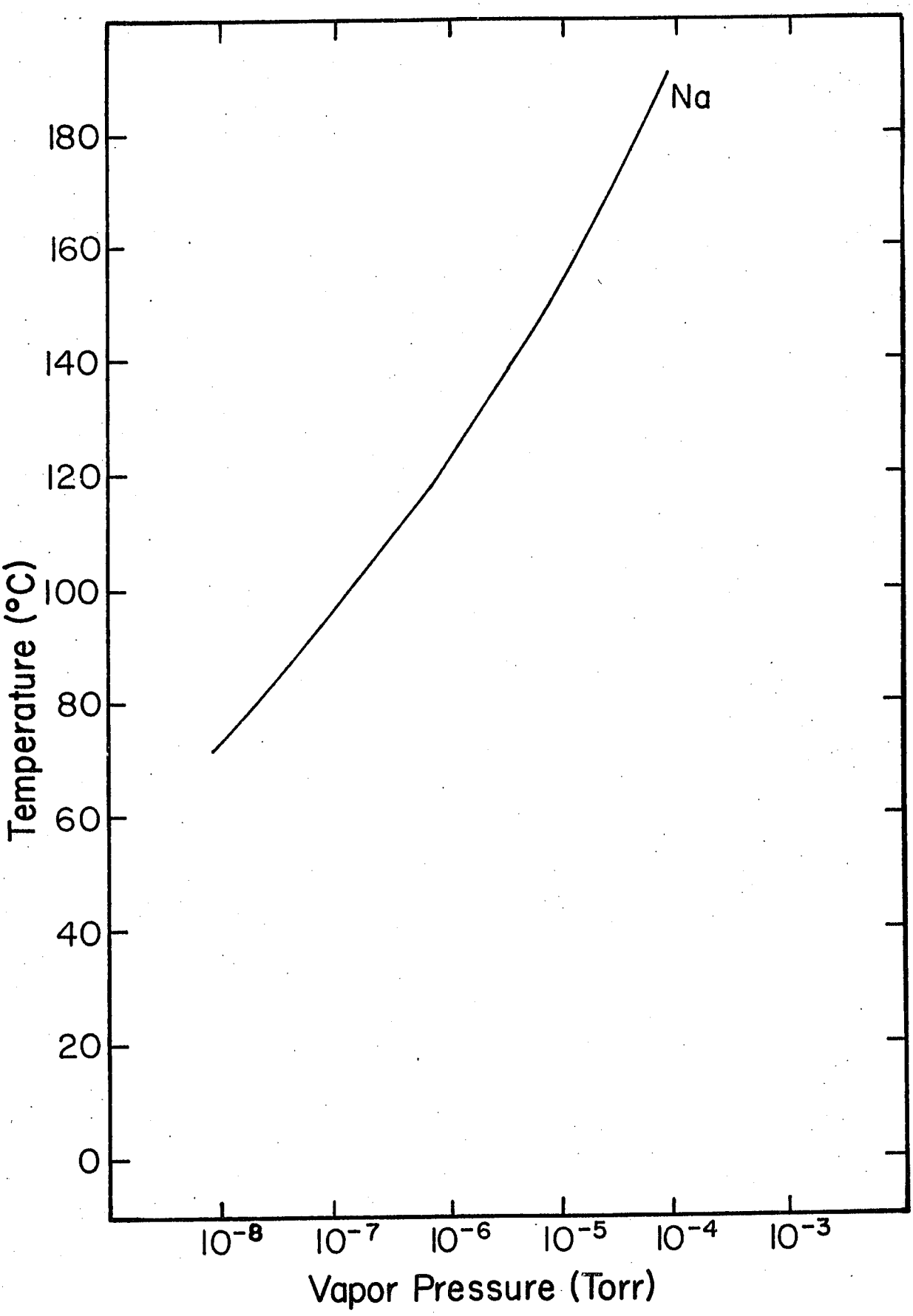
Na
180
160
140
120
100
80
60
40
20
0
Temperature (°C)
10^{-8}
10^{-7}
10^{-6}
10^{-5}
10^{-4}
10^{-3}
Vapor Pressure (Torr)

polarization of the pumping light. The measurements of the Zeeman transition were taken using the one-turn Helmholtz coil, while the NMR frequencies were measured using the six-turn coil and power amplifier.

In order to check whether the fluctuation of $g_I{}^+/g_J$ values was due to the systematic errors, a new run was begun by either reversing the field direction, changing the magnitude of the magnetic field, or slightly varying the position of the sample bulb and end caps. In other words, the condition and parameters of the entire system for the measurements were different from run to run, thus, we could easily identify the fluctuation of the g-factor ratio due to the systematic error or random error. The magnetic shields were demagnetized whenever the direction or magnitude of the magnetic field was changed.

5.2 ERROR ANALYSIS

1. Random Errors

In the calculation of $g_I{}^+/g_J$ from the NMR frequencies and Zeeman frequencies, the errors in g_I/g_J[11] and the hyperfine splitting of the Na are completely negligible.[11] Random errors arise from the measurements of NMR and Zeeman transitions. If we assume the uncertainties of each $g_I{}^+/g_J$ measurement are all equal and the parent population distribution is the Gaussian, the uncertainty of the $g_I{}^+/g_J$ data points δ can be estimated from the

data. Let X_i represents the ith point of g_I^+/g_J and N is the number of data points, which is much greater than 1. The standard deviation is

$$\sigma \approx \sqrt{\frac{\sum_i X_i^2}{N} - (\bar{X})^2} \quad ,^{69}$$

where $\bar{X} = \frac{\sum_i X_i}{N}$ is the average value of all X_i. If we neglect correlations between the X_i as well as second and higher-order terms in the expansion of the variance σ_μ^2 of the mean $\bar{X}$,[69] the random errors of each run can be expressed as the mean standard deviation

$$\sigma_\mu = \frac{\sigma}{\sqrt{N}} = \sqrt{\frac{\frac{\sum_i X_i^2}{N} - (\bar{X})^2}{N}} \quad .$$

By the same token, if there is no other source of error in the system except the random error, even varying the parameter of the system from run to run, one can also calculate the standard deviation as the error assign to the final mean g_I^+/g_J from each of all eleven runs by treating average g_I^+/g_J of each run as an individual data point.

2. Sources of Random Error

(1) Magnetic field drift

For most of the runs the Zeeman transition frequency

occurred at ~40 MHz and NMR occurred at a frequency of ~61 KHz when the applied static magnetic field was ~57 Gauss. The small variation of the field strength would result in a larger change in the frequency of the Zeeman transition than the NMR transition. However, this error resulted from the field drift would be almost eliminated by taking one determination of the NMR frequency sandwiched between two determinations of the Zeeman frequencies.

(2) The rf power line broadening of both NMR and Zeeman signals

There was the possibility of a rf power line broadening contributing to the line-widths of both the Zeeman transition[70] and the NMR resonance.[7] The line-width of the Zeeman signal relates to the strength of the rf field at the resonance frequency as (cf., 2.1)

$$\Delta\omega^2 = \frac{1}{\gamma_2^2} + \frac{\gamma_1}{\gamma_2}\omega_1^2$$

where $\Delta\omega$ is the line-width of the Zeeman signals.

γ_1 is a composite of the longitudinal relaxation times T_1^1, ... T_1^N due to N different relaxation mechanisms.

γ_2 is a composite of the transverse relaxation times T_2^1, ... T_2^N due to N different relaxation mechanisms.

ω_1 is the rf frequency.

However, fortunately the line broadening due to rf power

can be greatly reduced by decreasing the rf power to a level when the line-widths were minimum and the signals were still be able to be detected. All the measurements in this experiment were made at this minimum level of the rf power and the rf power contribution to the line-width would have been very small.

(3) The Zeeman line-width broadening due to the magnetic field

The major contribution to the line-width of the Zeeman frequency would be the inhomogeneity of the magnetic field over the volume of the 300 cc bulb. The width was ~400 Hz at the 57 Gauss of axial magnetic field, and is one of the principal parameters to determine the degree of the precision measurement of g_I^+/g_J.

(4) The NMR line-width broadening due to the inhomogeneity of the magnetic field

The NMR line-width contributed by the magnetic field can be roughly estimated from the Zeeman line-width together with either the value of g_I^+/g_J or the Zeeman and NMR frequencies. Their relation can be shown in the following

$$\Delta\nu_{NMR} = \frac{\Delta\nu_{Zeeman}}{\nu_{Zeeman}}\nu_{NMR} \simeq \Delta\nu_{Zeeman}\frac{4g_I^+}{g_J}$$

where $\Delta\nu_{NMR}$ is the NMR line-width due to the magnetic field.

$\Delta\nu_{Zeeman}$ is the Zeeman line-width due to the magnetic field.

ν_{NMR} is the NMR frequency.

ν_{Zeeman} is the Zeeman transition frequency.

Under the weak magnetic field approximation and neglecting the g_I term in the Hamiltonian, 4 in the above equation comes from the fact that the alkali g factor, including nuclear spins, relates to the g factor of the free electron as $g_F = \pm g_J/(2I + 1)$[71] for $F = I \pm 1/2$, and $I = 3/2$ for Na. The estimation of $\Delta\nu$ NMR is 0.64 Hz, compared with ~250 Hz of NMR total line-width of this experiment, which is relatively small.

(5) The NMR line-width broadening due to the charge-exchange collisions

Another important parameter of measuring g_I^+/g_J is the NMR line-width. Since we are dealing with the precision measurement of g_I^+/g_J, which is at least better than one part in 10^8, the NMR line-width should be required to be a narrow one. However, the width is ~250 Hz in this experiment, which is mostly contributed by the charge-exchange collision process.

3. Systematic Errors

Systematic errors are related to the incomplete knowledge of certain appropriate factors during the observations, and could not be calculated analytically. The principal source of systematic error in this experiment is the asymmetric line shape due to a combination of the inhomogeneities in the rf (H_1) and static (H_0) fields.[63] This is the most important parameter for the precision measurement of g_I^+/g_J.

CHAPTER VI

RESULTS, DISCUSSIONS, AND CONCLUSIONS

6.1 SUMMARY OF RESULTS

The results of our eleven final runs consisting of approximately 20 g-factor ratio measurements each are shown in Table 3. The mean standard deviation of the average g-factor ratio of each run is also included in Table 3. The mean standard deviation is calculated under the assumption that the errors are random (cf., 5.2). However, the variation in the results from run to run is larger than these errors predict. Our final g_I^+/g_J ratio is the average value from each of the eleven runs, and the assignment of the error to the final g-factor ratio would be the maximum spread in all the eleven g-factor ratios. The maximum spread is taken to be the standard deviation, and the distribution is assumed to be the Gaussian distribution. Thus, the final result is

$$\left[-4.01853 \pm 0.00015 \right] \times 10^{-4}$$

Comparing with the g-factor ratio of the neutral Na atoms $-4.0184406 \times 10^{-4}$,[11] it is obvious that there is no distinguishable difference between the g_I^+/g_J of the Na^+ ions and g_I/g_J of the Na atoms.

TABLE 3

Summary of the results of this experiment

No. of measurements	$g_I(^{23}Na^+)/g_J(^{23}Na) \times 10^{-4}$	Mean std. dev. $\times 10^{-4}$
20	-4.01860	0.00003
20	-4.01857	0.00002
20	-4.01851	0.00003
20	-4.01821	0.00003
20	-4.01847	0.00004
21	-4.01878	0.00005
21	-4.01875	0.00003
20	-4.01843	0.00003
20	-4.01853	0.00007
42	-4.01852	0.00005
25	-4.01841	0.00005

6.2 SOME THEORETICAL RESULT OF SHIELDING CONSTANT OF THE Na^+ IONS AND Na ATOMS

The nuclear g factor, g_I, for the ground state neutral Na atoms observed in rf spectroscopic experiments is less than the g factor, $\bar{g}_I$, of the bare nucleus, because of the diamagnetic shielding effect, and that the g_I and $\bar{g}_I$ are related as

$$g_I = (1 - \sigma)\ \bar{g}_I$$

where σ is the diamagnetic shielding constant for the ground state sodium atoms.

By the same token, for g_I^+ of the Na^+ ions would be

$$g_I^+ = (1 - \sigma^+)\ \bar{g}_I$$

where σ^+ is the diamagnetic shielding constant for the ground state positive Na^+ ions.

The difference of the shielding constant between the atoms and ions can be written

$$\sigma - \sigma^+ = \frac{(g_I^+ - g_I)}{\bar{g}_I}$$

We can rewrite the above equation as

$$\frac{g_I^+}{g_J} - \frac{g_I}{g_J} \simeq (\sigma - \sigma^+)\ \frac{g_I}{g_J}$$

since

$$\frac{\bar{g}_I}{g_J} \simeq \frac{g_I}{g_J}$$

This implies that the difference of shielding constants between the atoms and ions can be deduced from the differnece of g-factor ratios.

It is worthwhile to tabulate all the shielding constants of the Na and Na^+ even though there is an undistinguishable g-factor ratio between atoms and ions in this experiment. The shielding constant for the ground state Na atoms and Na^+ ions are listed in Table 4 and Table 5 respectively. From the Table 4 and 5, one can deduce $\sigma - \sigma^+$, and is 5.05×10^{-6} if σ and σ^+ are the values taken from the report of Malli and Fraga, 1966.[52] In turn, the $g_I^+/g_J - g_I/g_J$ value would be -2×10^{-9} which is very small.

6.3 DISCUSSION

The principal limitation of the precision measurements were the width and the assymmetric line shape of the NMR resonance. The assymmetric line shape was due to a combination of the inhomogeneities in the rf and static fields. The degree of homogeneity of the magnetic field in which the optical pumping cell situated could be improved by using the smaller cell. Unfortunately the smaller bulb we used, the smaller NMR signals we had. The width of the NMR signal was contributed mainly from the charge-exchange collisions. The way to reduce the line-width is to decrease the density of the Na atoms and hence reducing the number of collisions. However,

TABLE 4

Shielding constant of ground state Na atoms

References	Shielding constant $\times 10^{-4}$
Malli and Fraga[52]	+6.2887
Lamb[35]	+7.5529
Dickinson[13]	+6.29
Bonham and Strand[51] (Hartree-Fock)	+6.39087
Bonham and Strand[51] (Thomas-Fermi-Dirac)	+7.297

TABLE 5

Shielding constant of ground state Na^+ ions

References	Shielding constnat x 10^{-4}
Malli and Fraga[52]	6.2382
Dickinson[13]	6.2371

the intensity of the NMR signal depends upon the polarization and number of the Na atoms. In other words, there is an optimum value between parameters of the NMR line-width and the size of the NMR signal. In the conventional optical pumping experiment, there would be an interference filter to filter out the D2 line to increase the efficiency of the pumping process. However, this is not the case for this experiment since the sodium D lines are too close to utilize the filter effectively. The advantage of a large degree of polarization of the Na atoms is two-fold: 1) to produce a strong NMR signal so one could afford to narrow the NMR line-width by reducing the number of atoms in the sample cell; 2) to produce a big Zeeman signal so that one could afford to narrow the width of the Zeeman signal by decreasing the cell volume, there-by reducing the inhomogeneity of the magnetic field.

The other difficulty of this experiment arose from the fact that sodium blackens glass, preventing the use of a conventional rf light source which would supply a smaller and quieter noise background.

6.4 CONCLUSION

Although the NMR signal of the Na^+ ions has been observed, the value of g_I/g_J lies within an error bar of the g_I^+/g_J. The undistinguishable result of g-factor ratios between Na and Na^+ afford us no information on

the difference of the diamagnetic shielding constnats between the atoms and ions unless the difficulties of this experiment stated in the above section are overcome.

It was suggested that the use of a higher static magnetic field strength should increase the precision of the measured value of g_I^+/g_J by reducing the fractional line-width of the NMR signal.[7]

BIBLIOGRAPH

1. A. Kastler, J. Phys. Radium 11, 255 (1950).

2. H. G. Dehmelt, Phys. Rev. 109, 381 (1958).

3. J. K. Mitchell, and E. N. Fortson, Phys. Rev. Lett., 21, 1621 (1968).

4. J. K. Mitchell, and E. N. Fortson, Phys. Rev. A 8, 704 (1973).

5. A. F. Oluwole, and E. A. Togun, J. Phys. B: Atom. Molec. Phys. 6, L334, (1973).

6. H. Nienstadt, G. Schmidt, S. Ullrich, H. G. Weber, and G. Zu Putlitz, Phys. Lett. A 41, 249 (1972).

7. S. J. Davis, J. J. Wright, and L. C. Balling, Phys. Rev. A 9, 1494, (1974).

8. C. E. Moore, Atomic Energy Level (National Bureau of Standards) Vol. I (1949), Vol. II (1952), and Vol. III (1958).

9. J. J. Wright, Ph. D. Dissertation, University of New Hampshire, 1969 (unpublished) P. 2.

10. L. C. Balling, Optical Pumping, Advances in Quantum Electronics, Vol. III (Academic Press Inc., London, 1975) P. 2.

11. A. Beckmann, K. D. Böklen, and D. Elke, Z Physik 270, 173 (1974).

12. E. Hylleraas and S. Skavlem, Phys. Rev. 79, 117 (1950).

13. W. C. Dickinson, Phys. Rev. 80, 563 (1950).

14. G. Herzberg, Atomic Spectra and Atomic Structure, (Dover Publications, New York, 1945) 2nd Edition.

15. R. B. Leighton, Principles of Modern Physics, (McGraw-Hill Book Company, New York, 1959) P. 208.

16. R. A. Bernheim, Optical Pumping, (W. A. Benjamin, New York, 1965) P. 6.

17. L. I. Schiff, Quantum Mechanics, (McGraw-Hill Book Company, New York, 1968) 3rd Edition P. 414.

18. R. L. deZafra, Am. J. Phys. 28, 646 (1960).

19. A. Gallagher, Phys. Rev. 157, 68 (1967); 163, 206 (1967).

20. S. M. Jarrett, Phys. Rev. 133, A 111 (1964).

21. H. G. Dehmelt, Phys. Rev. 105, 1487 (1957).

22. A. E. Siegman, An Introduction to Lasers and Masers, (McGraw-Hill Book Company, New York, 1971) P. 142.

23. L. C. Balling, Optical Pumping, Advances in Quantum Electronics, Vol. III (Academic Press Inc., London, 1975) P. 11.

24. W. Franzen and A. G. Emslie, Phys. Rev. 108, 1453 (1957).

25. C. P. Slichter, Principles of Magnetic Resonance, (Harper and Row, New York, 1963) P. 18.

26. A. E. Siegman, An Introduction to Lasers and Masers, (McGraw-Hill Book Company, New York, 1971) P. 147.

27. J. A. R. Samson and G. L. Weissler, "Absorption Photoionization, and Scattering Cross Sections", in Methods of Experimental Physics, ed. by B. Bederson and W. L. Fite (Academic Press Inc., New York, 1968). Vol. 7A, P. 143.

28. G. Breit and I. I. Rabi, Phys. Rev. 38, 2082 (1931).

29. H. V. Buttlar, Nuclear Physics, An Introduction, (Academic Press Inc., New York, 1968) P. 257.

30. H. Kopfermann, Nuclear Moments, (Academic Press Inc., New York, 1958) P. 26.

31. B. L. Bean, Ph. D. Dissertation, University of New Hampshire, 1975 (Unpublished) P. 11.

32. L. C. Balling, Optical Pumping, (Advances in Quantum Electronics, Vol. III, Academic Press Inc, London, 1975) P. 13.

33. H. A. Bethe and R. W. Jackiw, Intermediate Quantum Mechanics (W. A. Benjamin, New York 1968). 2nd ed., P. 10.

34. E. U. Condon and G. H. Shortley, The Theory of Atomic Spectra (University Press, Cambridge, 1953), P. 63.

35. W. E. Lamb, Phys. Rev. 60, 817 (1941).

36. N. F. Ramsey, Phys. Rev. 77, 567 (1950).

37. N. F. Ramsey, Phys. Rev. 78, 699 (1950).

38. N. F. Ramsey, Phys. Rev. 86, 243 (1952).

39. N. F. Ramsey, Molecular Beams (Oxford University Press, London, 1955) P. 162.

40. L. Armstrong, Theory of the Hyperfine Structure of Free Atoms (Wiley-Interscience, New York, 1971) P. 129.

41. L. H. Thomas, Proc. Cambridge Phil. Soc. 23, 542 (1927).

42. E. Fermi, Z. Physik 48, 73 (1928).

43. E. U. Condon and G. H. Shortley, The Theory of Atomic Spectra (University Press, Cambridge, 1953), P. 336.

44. L. I. Schiff, Quantum Mechanics, (McGraw-Hill Book Company, New York, 1968) 3rd Edition, P. 430.

45. R. M. Eisberg, Fundamentals of Modern Physics (John Wiley and Sons, Inc., New York, 1961), P. 393.

46. V. Bush, and S. H. Caldwell, Phys. Rev. 38, 1898 (1931).

47. J. D. Jackson, Classical Electrodynamics, (John Wiley and Sons, Inc., New York, 1962) P. 146.

48. H. A. Bethe and R. Jackiw, Intermediate Quantum Mechanics, (W. A. Benjamin Inc., Mass. 1968), Second Edition, P. 56.

49. J. C. Slater, Quantum Theory of Atomic Structure, (McGraw-Hill Book Company, New York, 1960), Vol. II, P. 4.

50. H. Kopfermann, Nuclear Moments (Academic Press Inc., New York, 1958) P. 158.

51. R. A. Bonham and T. G. Strand, J. Chem. Phys. 40, 3447 (1964).

52. G. Malli and S. Fraga, Theor. Chem. Acta 5, 275 (1966).

53. W. Happer, Rev. Mod. Phys. 44, 169 (1972).

54. GE Na-1 Light Bulb could be Purchased from V. W. R., Box 232 Boston, Mass. 02102.

55. S. J. Davis, Ph. D. Dissertation, University of New Hampshire, 1973 (Unpublished) P. 42.

56. F. A. Jenkins, and H. E. White, Fundamentals of Optics, (McGraw-Hill, New York, 1957) 3rd Edition, P. 557.

57. M. Francon, Optical Interferometry, (Academic Press Inc., New York and London, 1966) P. 124.

58. A. C. G. Mitchell and M. W. Zemansky, Resonance Radiation and Excited Atoms, (MacMillan, Cambridge, England, 1934) P. 21.

59. R. A. Bernheim, Optical Pumping: An Introduction (W. A. Benjamin, Inc., New York, 1965) P. 22.

60. B. L. Bean, Ph. D. Dissertation, University of New Hampshire, 1975 (Unpublished) P. 55.

61. R. J. Hanson and F. M. Pipkin, Rev. Sci. Inst. 36, 179 (1965).

62. L. C. Balling, Optical Pumping, Advances in Quantum Electronics, Vol. III (Academic Press Inc., London, 1975) P. 154.

63. C. W. White, W. M. Hughes, G. S. Hayne, and H. G. Robinson, Phys. Rev. 174, 23 (1968).

64. RCA Phototubes and Photocells, Technical Manual PT-60 P. 111.

65. Anderson Glass Company, Old Turnpike Road, Fitzwilliam, New Hampshire, 03447.

66. Na Ampoules could be Purchased from Leico Industries Inc., 250 W. 57th St. New York, N. Y. 10019.

67. Linde Specialty Gases Purchased from Welders Supply Company, Inc., 128 Wheeler Road, Burlington, Mass. 01803.

68. R. E. Honig, RCA Review, 23, 574 (1962).

69. P. R. Bevington, Data Reduction and Error Analysis for the Physical Sciences, (McGraw-Hill Book Company, New York, 1969) P. 70.

70. L. C. Balling, Optical Pumping, Advances in Quantum Electronics, Vol. III (Academic Press, London, 1975) P. 59.

71. L. C. Balling, Optical Pumping, Advances in Quantum Electronics, Vol. III (Academic Press Inc., London, 1975) P. 14.

Appendix A

Derivation of the Formula for the Calculation of $g_I(^{23}Na^+)/g_J(^{23}Na)$

From the Breit-Rabi formula, a known g_I/g_J and hyperfine splitting of the neutral Na atoms, together with a Zeeman and NMR frequency at a static magnetic field along the z-axis, we could come up with a formula for the calculation of g_I^+/g_J. The derivation is the following:

The energy levels in the ground states of Na in the F, M representation as a function of an applied static magnetic field are given by the Breit-Rabi formula,

$$E_{F,M} = -\frac{\Delta W}{2(2I+1)} - g_I \mu_0 H_0 M \pm \frac{\Delta W}{2}\sqrt{1+\frac{4M}{2I+1}X+X^2} \quad ,$$

where $\Delta W = \frac{hA}{2}(2I+1)$, which is the hyperfine splitting

$$X = \frac{(-g_J + g_I)\mu_0 H_0}{\Delta W} \qquad (A\cdot 1)$$

$g_J\mu_0 = \mu_J/J$

$g_I\mu_0 = \mu_I/I$

μ_0 is the Bohr Magneton.

μ_J is the electronic magnetic moment.

μ_I is the nuclear magnetic moment.

$\pm$ signs apply for $F = I \pm 1/2$ and $I = 3/2$ for Na.

If we take the largest energy separation between the $F = 2$, $M = -1$ and $F = 2$, $M = -2$ Zeeman levels, and from the

Breit-Rabi formula, the Zeeman frequency can be written

$$f_1 = -\frac{g_I \mu_0 H_0}{h} + \frac{\Delta W}{2h}\left(\sqrt{1 - X + X^2} - 1 + X\right) \quad .$$

Rewrite the above equation, we get

$$-\frac{g_I \mu_0 H_0}{h} = f_1 - \frac{\Delta W}{2h}\left(\sqrt{1 - X + X^2} - 1 + X\right) \quad . \qquad (A.2)$$

From the Equation (A.1) and (A.2), we have

$$-\frac{g_J \mu_0 H_0}{h} = f_1 - \frac{\Delta W}{2h}\left(\sqrt{1 - X + X^2} - 1 - X\right) \quad . \qquad (A.3)$$

By the use of the Equation (A.1), we also have

$$-\frac{g_J \mu_0 H_0}{h} = \frac{\Delta W X}{h\left[1 - \frac{g_I}{g_J}\right]} \quad . \qquad (A.4)$$

The goal is to set up an equation of $-g_J \mu_0 H_0/h$, and solve for it in terms of $\Delta W/h$, g_I/g_J and Zeeman frequency f_1. For simplicity, let $Y = -g_J \mu_0 H_0/h$, and $A = g_I/g_J$ and from (A.3) and (A.4) we could set up a quadratic equation of $-g_J \mu_0 H_0/h$ by cancelling X. The equation becomes

$$AY^2 - \left[\frac{\Delta W}{4h}(1+3A) + f_1(1+A)\right]Y + f_1\left(f_1 + \frac{\Delta W}{h}\right) = 0 \qquad (A.5)$$

Solving for Y in terms of f_1, ΔW, and A; the solution is

$$Y = \frac{1}{2A}\left\{\left[\frac{\Delta W}{4h}(1+3A) + f_1(1+A)\right] - \sqrt{\left[\frac{\Delta W}{4h}(1+3A) + f_1(1+A)\right]^2 - 4Af_1\left(f_1 + \frac{\Delta W}{h}\right)}\right\} \qquad (A.6)$$

Here we take "-" sign, since Y is positive, and A is negative.

The NMR frequency of the ion f_2 can be expressed as

$$f_2 = -\frac{g_I^+ \mu_0 H_0}{h} \quad , \qquad (A.7)$$

where g_I^+ is the g factor for the Na^+ ions.

Then from equations (A.6) and (A.7) we get

$$\frac{g_I^+}{g_J} = \frac{f_2}{Y} = 2Af_2\left\{\left[\frac{\Delta W}{4h}(1+3A)+f_1(1+A)\right]-\sqrt{\left[\frac{\Delta W}{4h}(1+3A)+f_1(1+A)\right]^2-4Af_1\left(f_1+\frac{\Delta W}{h}\right)}\right\}^{-1} \quad (A\cdot 8)$$

There is another way to get g_I^+/g_J simply let $f_3 = f_1 - AY = f_1 + g_I\mu_0 H_0/h$, and set up an equation of Y and solve for Y in terms of $\Delta W/h$, A, and f_3. From equation (A.2) we get

$$f_3 = \frac{\Delta W}{2h}\left(\sqrt{1-X+X^2} - 1 + X\right) . \quad (A\cdot 9)$$

Again use equation (A.4) to eliminate X of equation (A.9), and take the square and rearrange it, we have

$$(1-A)Y\left(\frac{\Delta W}{4h}+f_3\right) = f_3\left(f_3+\frac{\Delta W}{h}\right) .$$

The solution of the above equation is

$$Y = \frac{f_3\left(f_3+\frac{\Delta W}{h}\right)}{(1-A)\left(\frac{\Delta W}{4h}+f_3\right)} . \quad (A\cdot 10)$$

Combining equations (A.7) and (A.10), finally we have

$$\frac{g_I^+}{g_J} = \frac{f_2(1-A)\left(\frac{\Delta W}{4h}+f_3\right)}{f_3\left(f_3+\frac{\Delta W}{h}\right)} \quad (A\cdot 11)$$

Equations (A.8) and (A.11) are the equation which would be used for the calculation of g_I^+/g_J.

Appendix B

Computer program for the Calculation of $g_I(^{23}Na^+)/g_J(^{23}Na)$

This program is designed to be used on the terminal for calculating g_I^+/g_J. Double precision is used since we need to know a small change of the g-factor ratio, about the order of one part in 10^8, between sodium atoms and ions. This program reads data either from typing or a set of data files stored in the computer. A Zeeman frequency; (F = 2, M = -1↔F = 2, M = -2); and a NMR frequency of Na^+ are taken for the calculation of each g_I^+/g_J.

As we have shown in Appendix A, there are two ways to calculate g_I^+/g_J. Thus the average g-factor ratios and their standard deviations, based on both calculations, would be given explicitly.

The physical quantity of each notation used in this program are shown as follows:

F1 is the Zeeman frequency between energy levels F = 2, M = -1, and F = 2, M = -2 of the ground state Na atoms.

F2 is the NMR frequency of the ground state Na^+ ions.

R1 and R2 stand for g_I^+/g_J based on equations (A.8) and (A.11) in Appendix A respectively.

Y is $-g_J\mu_0H_0/h$.

F3 = F1 + $g_I\mu_0H_0/h$.

H is hyperfine splitting in frequency unit (Hz).

A is g_I/g_J of the ground state neutral Na atoms and it is a negative number.

Notice that we designate A = 4.0184406×10^{-4} as a positive number in this program for the convenience of calculations. Thus the formulas of g_I^+/g_J would have to set -A = A in order to get the exact expression as these equations of Appendix A.

This program is shown as follows:

```
LEVEL 0
100         REAL*8 F1(222),F2(222),P1(222),P2(222),Y
110         REAL*8 A,B,C,E,F3
120         REAL*8 SR11,SR12,SR21,SR22,SR1,SR2,FN,FNS
125         REAL*8 FNAM,STAR
130         REAL*4 YES,NO
140         INTEGER*4 IDEL(25)
150         DATA YES,NO,STAR/'Y','N','*'/
160         DATA A/4.0184406D-4/
170         DATA ID/1/
180         WRITE(6,110) ID
190 110     FORMAT('+HYPERFINE SPLITTING=',A4)
200         READ(5,*) F
210         WRITE(6,140) ID
220 140     FORMAT('+DATA IN A FILE',A4)
230 9       READ(5,150) ANS
240 150     FORMAT(A1)
250         IF(ANS.EQ.YES) GO TO 10
260         IF(ANS.EQ.NO) GO TO 11
270         WRITE(6,160)
280 160     FORMAT('+INCORRECT ENTRY: ANSWER YES OR NO')
290         GO TO 9
300 10      WRITE(6,170) ID
310 170     FORMAT('+FILE NAME',A4)
320         READ(5,*) FNAM
330         CALL OPEN(1,FNAM,'INPUT')
340         READ(1) FN1,FN2
350         N=FN1
360         WRITE(6,180) N
370 180     FORMAT('+NUMBER OF DATA POINTS=',A4)
380         DO 12 I=1,N
390 12      READ(1) F1(I),F2(I)
400         CALL CLOSE(1)
410         GO TO 4
420 11      WRITE(6,100) ID
430 100     FORMAT('+NUMBER OF DATA POINTS=',A4)
440         READ(5,*) N
450         WRITE(6,120)
460 120     FORMAT('+F1,F2=')
```

```
      DO 1 I=1,N
    1 READ(5,*)F1(I),F2(I)
    4 WRITE(6,200) ID
  200 FORMAT('+DATA LISTING',A4)
      READ(5,150) ANS
      IF(ANS.EQ.NO) GO TO 20
      DO 21 I=1,N
   21 WRITE(6,210) I,F1(I),F2(I)
  210 FORMAT(1X,I4,1X,G22.16,1X,G22.16)
      WRITE(6,290)
  290 FORMAT(/)
   20 WRITE(6,220) ID
  220 FORMAT('+CHANGES',A4)
      READ(5,150) ANS
      IF(ANS.EQ.NO) GO TO 30
      WRITE(6,230) ID
  230 FORMAT('+NUMBER OF POINTS YOU WANT TO REMOVE',A4)
      READ(5,*) NDEL
      IF(NDEL.EQ.0) GO TO 22
      WRITE(6,240) ID
  240 FORMAT('+ENTER POINTS',A4)
      READ(5,*) (IDEL(I),I=1,NDEL)
      DO 23 K=1,NDEL
      IPT=IDEL(K)
      N=N-1
      DO 24 I=IPT,N
      F1(I)=F1(I+1)
   24 F2(I)=F2(I+1)
      DO 23 J=K,NDEL
      IF(IDEL(J).GT.IPT) IDEL(J)=IDEL(J)-1
   23 CONTINUE
   22 WRITE(6,250) ID
  250 FORMAT('+HOW MANY POINTS DO YOU WANT TO ADD',A4)
      IF(NADD.EQ.0) GO TO 29
      WRITE(6,260)
  260 FORMAT('+F1,F2=')
      DO 25 I=1,NADD
      N=N+1
   25 READ(5,*) F1(N),F2(N)
   29 GO TO 4
   30 WRITE(6,270) ID
  270 FORMAT('+OUTPUT FILE NAME (ENTER ''*'' FOR NO FILE)',A4)
      READ(5,*) FNAM
      IF(FNAM.EQ.STAR) GO TO 5
      CALL OPEN(2,FNAM,'OUTPUT')
      FN1=N
      FN2=2.
      WRITE(2) FN1,FN2
      DO 26 I=1,N
   26 WRITE(2) F1(I),F2(I)
      CALL CLOSE(2)
    5 DO 2 I=1,N
      B=-(2.5D-1)*H*(1.0D0-3.0D0*A)-F1(I)*(1.0D0-A)
      C=-F1(I)*(H+F1(I))
      Y=(B+DSQRT(B*B-4.0D0*A*C))/(2.0D0*A)
      R1(I)=F2(I)/Y
```

```
1020      F3=R1(I)+A*Y
1030      R2(I)=R2(I)*(1.0D0+A)*(2.5D-1*H+F3)/(F3*(H+F3))
1031      WRITE(6,300) R2(I)
1032  300 FORMAT(' ',F30.25)
1040    2 CONTINUE
1050      FN=N
1060      FNS=DSQRT(FN)
1070      SR11=0.D0
1080      SR12=0.D0
1090      SR21=0.D0
1100      SR22=0.D0
0110      DO 3 I=1,N
1120      SR11=SR11+R1(I)
1130      SR12=SR12+R1(I)*R1(I)
1140      SR21=SR21+R2(I)
1150    3 SR22=SR22+R2(I)*R2(I)
1160      SR11=SR11/FN
1170      SR12=SR12/FN
1180      SR21=SR21/FN
1190      SR22=SR22/FN
1200      SR1=DSQRT(SR12-SR11*SR11)/FNS
1210      SR2=DSQRT(SR22-SR21*SR21)/FNS
1220      WRITE(6,130) SR11,SR1,SR21,SR2
1230  130 FORMAT(' RATIO 1 =',F30.25,/12X,'STD DEV =',G22.16%
1240     /' RATIO 2 =',F30.25,/12X,'STD DEV =',G22.16/)
1250      WRITE(6,280) ID
1260  280 FORMAT(' RECYCLE',A4)
1270      READ(5,150) ANS
1280      IF(ANS.EQ.YES) GO TO 4
1290      END
```